Complementary Nuclear Magnetic Resonance-Based Metabolomics Approaches for Glioma Biomarker Identification in a Drosophila melanogaster Model

Marion Maravat, Marylène Bertrand, Céline Landon, Franck Fayon, Séverine Morisset-Lopez, Vincent Sarou-Kanian, Martine Decoville

▶ **To cite this version:**

Marion Maravat, Marylène Bertrand, Céline Landon, Franck Fayon, Séverine Morisset-Lopez, et al.. Complementary Nuclear Magnetic Resonance-Based Metabolomics Approaches for Glioma Biomarker Identification in a Drosophila melanogaster Model. Journal of Proteome Research, 2021, 20 (8), pp.3977-3991. 10.1021/acs.jproteome.1c00304 . hal-03335927

HAL Id: hal-03335927
https://hal.science/hal-03335927v1

Submitted on 22 Nov 2021

HAL is a multi-disciplinary open access archive for the deposit and dissemination of scientific research documents, whether they are published or not. The documents may come from teaching and research institutions in France or abroad, or from public or private research centers.

L'archive ouverte pluridisciplinaire **HAL**, est destinée au dépôt et à la diffusion de documents scientifiques de niveau recherche, publiés ou non, émanant des établissements d'enseignement et de recherche français ou étrangers, des laboratoires publics ou privés.

Complementary NMR-based metabolomics approaches for glioma biomarker identification in a *Drosophila melanogaster* model

Marion Maravat[1], Marylène Bertrand[2], Céline Landon[2], Franck Fayon[1], Séverine Morisset-Lopez[2], Vincent Sarou-Kanian[1], Martine Decoville[2*]

[1] *CNRS, CEMHTI UPR3079, Université d'Orléans, F-45071, Orléans, France*

[2] *CNRS, CBM UPR4301, Université d'Orléans, F-45071, Orléans, France*

* *Corresponding author : martine.decoville@cnrs-orleans.fr*

Abstract

Human malignant gliomas are the most common type of primary brain tumors. Composed of glial cells and their precursors, they are aggressive and highly invasive, leading to a poor prognosis. Due to the difficulty of surgically removing tumors and their resistance to treatments, novel therapeutic approaches are needed to improve patient life expectancy and comfort.

Drosophila melanogaster is a compelling genetic model to better understanding human neurological diseases thanks to its high conservation in signaling pathways and cellular content of the brain. Here, glioma has been induced in *Drosophila* by co-activating the Epidermal Growth Factor Receptor (EGFR) and the Phosphatidyl-Inositol-3 Kinase (PI3K) signaling pathways.

Complementary nuclear magnetic resonance (NMR) techniques were used to obtain metabolic profiles in third instar larvae brains. Fresh organs were directly studied by ^{1}H High Resolution – Magic Angle Spinning (HR-MAS) NMR and brain extracts were analyzed by solution-state ^{1}H-NMR. Statistical analyses revealed differential metabolic signatures, impacted metabolic pathways and glioma biomarkers. Each method was efficient to determine biomarkers. The highlighted metabolites including glucose, myo-inositol, sarcosine, glycine, alanine and pyruvate for solution-state NMR and proline, myo-inositol,

acetate and glucose for HR-MAS, show very good performances in discriminating samples according to their nature with data mining based on ROC curves. Combining results allows for a more complete view of induced disturbances and opens the possibility of deciphering the biochemical mechanisms of these tumors. The identified biomarkers provide a means to rebalance specific pathways through targeted metabolic therapy and to study the effects of pharmacological treatments using *Drosophila* as a model organism.

Keywords : *Drosophila*, glioma, HR-MAS, metabolism, NMR.

1. Introduction

Malignant gliomas represent 50% of tumors of the central nervous system and are characterized by the destructive, fast and diffuse proliferation of glial cells [1]. Gliomas were first classified based on the type of glial cells they are originated from (astrocytes, oligodendrocytes or ependymal cells) and then ranked from grade I to IV based on their malignancy [1, 2]. Recently additional phenotypic and genetic parameters have been considered by the World Health Organization (WHO) to refine the classification of diffuse gliomas, including the WHO grade II and III astrocytic tumors, the grade II and III oligodendrogliomas and the grade IV glioblastoma multiform (GBMs) [3].

GBMs are the most aggressive gliomas and the median survival time of patients is 15 to 16 months [4]. GBM cells are characterized by their diffuse infiltration into healthy brain tissue which renders complete surgical resection impossible and they show high resistance to apoptosis making chemotherapy and radiotherapy unsuccessful [1, 5, 6]. The development of new therapeutic approaches to improve patients' life expectancy and comfort are thus highly needed.

GBM present heterogeneity in terms of genetic alterations inside the same tumor [7]. In most GBM cases, a Receptor Tyrosine Kinase (RTK) called Epidermal Growth Factor Receptor (EGFR) and its downstream signaling network are altered [3, 8]. Besides mutations in genes encoding isocitrate dehydrogenases 1 and 2 (IDH1 and IDH2) are also found in Low Grade Gliomas (grades II and III) and secondary GBMs (GBM, IDH-mutant) [3]. In 40 % of exclusively primary GBMs, the wild-type EGFR gene is amplified resulting in

EGFR overexpression [2, 9-11]. In addition, in 50 to 60% of the EGFR amplified primary GBMs, the presence of an EGFR variant allele known as EGFRvIII (or ΔEGFR or del2-7EGFR) has been detected. This receptor mutant generated from a deletion in the extracellular domain becomes unable to bind ligands but exhibits constitutive activity, therefore increasing cell proliferation [12, 13]. Aberrant EGFR's signaling cascade including effectors regulating cell proliferation and apoptosis can also be altered in gliomas [1, 8]. The two main are the RAS/MAPK pathway which regulates cell proliferation and the Phosphatidylinositide 3 Kinase (PI3K)-AKT-mTOR pathway, which controls cell survival and proliferation. Gain of function mutation in PIK3CA which codes for the catalytic subunit p110α of the enzyme PI3K has been reported in 15% of GBMs [14, 15]. Overexpression of the wild type form of *PI3KD* gene has been described in GBMs [16, 17]. In some cases, activation of the PI3K pathway has been associated with expression of the EGFRvIII variant or loss of the tumor suppressor Phosphatase TENsin homolog (PTEN). EGFRvIII expression has been associated with PI3K activation, the tumor suppressor PTEN being inhibited or not [18]. Inhibitors targeting EGFR or mTOR have been used to treat GBMs but demonstrate no effect or only a cytostatic one [8, 19, 20].

Metabolic reprogramming in cancer cells is a well-known hallmark of carcinogenesis even if the mechanisms are not fully understood yet and they differ between different types of cancers [21-23]. Cancer cells need to modify their metabolic pathways in order to produce energy and to proliferate. These modifications are not restricted to one pathway at the time but rather work as a whole to respond to the cancer cell's needs to proliferate and survive. Glioma cells, as many other cancer cells, use aerobic glycolysis known as the Warburg effect [24]. Cancer cell glucose intake increases and its product pyruvate is converted to lactate through fermentation instead of going through the Tricarboxylic Acid Cycle (TCA cycle) and oxidative phosphorylation (OXPHOS) for adenosine triphosphate (ATP) production [25]. This phenomenon is independent of the amount of oxygen. Although aerobic glycolysis is less productive in terms of number of ATP than the oxidative metabolism, its higher rates promotes faster energy production to compensate [24-26]. The increased levels of produced lactate acidify the extracellular environment and provide biomass resources to stimulate cell proliferation [26, 27]. Aerobic glycolysis not only generates lactate and energy for proliferation but also intermediates necessary for synthesis of

amino acids, nucleotides and fatty acids [23]. Pyruvate being preferentially converted to lactate, the Tricarboxylic Acid Cycle (TCA cycle) is also altered to maintain mitochondrial function [23]. Anaplerotic pathways produce intermediate metabolites to replenish the cycle so that biomass precursors like amino acids can still be synthesized [23]. It has been shown that glioma cells can also use fatty acids and ketones to provide acetyl CoA which can then feed the TCA cycle and OXPHOS [25, 27]. Lastly, the Pentose Phosphate Pathway (PPP) is reported to be very active compared to glycolysis in dividing glioma cells in order to produce nucleotides necessary for nucleic acid replication [27, 28]. Modification of the metabolism in glioma cells is not well understood, but it is often tightly linked to genetic alterations: for example alteration in the RTK/PI3K/AKT/mTOR pathway, which regulates glucose and glutamine metabolism [29] and mutations in Isocitrate Dehydrogenase (IDH1/2), which lead to production of the oncometabolite D-2-hydroxyglutarate (D-2HG) [30, 31].

Metabolic changes are usually a consequence of the genetic mutations that cause gliomas. However they are essential not only for tumor growth but also for responding to changes in the microenvironment. It is of particular importance in the case of gliomas as they develop in the brain where the different cell types (neurons, astrocytes, microglia) are in close interactions, influencing each other. Targeting such altered metabolic adaptations migth enable the development of new therapeutic approaches . Moreover, identification of metabolic signatures in gliomas may be used as diagnostic biomarkers to refine the classification of the different grades [33] and thus for early detection of glioblastomas. They also may be helpful to follow the response to therapy. Therefore*, in vivo* GBMs models are useful for such studies by allowing to take into consideration the importance of interaction between different cell types in the brain, and adaptation of the glioma metabolism to its microenvironment [32].

Recently, two glioma models have been developed in *Drosophila*, mirroring the main characteristics of human gliomas. There are many advantages in using *Drosophila melanogaster* as a model organism for human diseases. On a practical side, it is relatively cost and time effective with a generation time of 12 days at 26°C. Moreover, manipulation of gene expression in *Drosophila* is easily achievable with the binary system Gal4/UAS. Regarding its usefulness to study human pathologies, *Drosophila* is known to

possess homolog genes for more than 65% of known human genes causing diseases [34]. Considering the high conservation of signaling and metabolic pathways, this fly is a compelling model to study human diseases and in particular cancer [35, 36].

A first model, established by Read et al. in 2009 [37] and used in this study, is based on the co-expression of constitutive forms of PI3K and EGFR in glial cells during larval development. This induces abnormal glial proliferation similar to human glioma, deformed and larger brains, and lethality during the 3rd instar larval stage [37, 38]. A second model was recently developed in adult by co-activating the PI3K and EGFR signaling pathway only in adult brain [39]. These two *in vivo* models are of particular interest to explore alterations in metabolism, because they maintain the interaction between glial cells and neurons.

NMR spectroscopy is a first-line analytical method in metabolomics, applicable to liquid and to semi-solid samples. Solution-state NMR is recognized as a method of choice for biomarker identification, due to its high resolution and its high reproducibility. However, even if it requires little sample preparation, the metabolite extraction step could induce biases, and the results obtained *in vitro* could not fully reflect biochemical mechanisms observed *in vivo.* Usually showing lower resolution and sensitivity than solution-state NMR, ^{1}H HR-MAS is much less used. Nevertheless, it has the great advantage to require minimum sample preparation and for example, analyses were here directly performed on intact larval brains (*ex vivo*). The HR-MAS technique is thus considered as an essential bridge between *in vivo* and tissue-extract NMR spectroscopy [40]. However while many studies compare *in vivo* and *ex vivo* data, only a few of them rely on the comparison of *ex vivo* HR-MAS and *in vitro* solution-state NMR data [40-42] as recently brilliantly illustrated to monitor differentiations of stem cells [42].

Metabolomic studies using NMR spectroscopy has already been succesfully used in *Drosophila* to characterize specific metabolites involved in various physiological processes : effect of environmental conditions temperature [43-49], dessication and starvation [50], effect of hypoxia [51-54]or infection [55] and also in disease models such as Huntington disease [56, 57] or Alzheimer disease [58]). Several HR-MAS studies were also conducted in *Drosophila* and have demonstrated the relevance of this technique to identify metabolic modifications in various biological conditions: response to trauma [59, 60] or *Drosophila* mutants and disease models [60-62]. The main goal of this study is therefore to explore the metabolic modifications linked to the

induction of glioma in a *Drosophila* larval model by combining two complementary techniques, ^{1}H solution-state and HR-MAS NMR.

2. Material and methods

2.1 Drosophila culture

The fly stocks were maintained at 22°C on a standard medium (per liter: 90.25 g cornmeal, 82.5 g dry yeast, 10.75 g agar and 37.5 mL of a 10% solution of methyl-4-hydroxybenzoate in ethanol). Crosses were performed at 26°C on standard medium. *Drosophila* lines were obtained from the Bloomington Stock Center except the stock UAS-dEGFR$^{\lambda}$ (T. Schubach).

Glioma were generated by crossing *UAS-dp110^{CAAX}; UAS-dEGFR$^{\lambda}$* virgins with *UAS-GFP; repo-Gal4/TMTbSb* males. As controls, we crossed UAS-dp110^{CAAX}; UAS-dEGFR$^{\lambda}$ virgins with *w^{1118}* males (UAS controls) and *w*^{1118} virgins with *UAS-GFP; repo-Gal4/TMTbSb* (*Gal4* controls) males. Larval brains were recovered from 3rd instar wandering larvae (120 hrs a.e.d.).

2.2 NMR spectroscopy experiments

Solution-state ^{1}H-NMR analysis

Third instar larval brains were dissected following the same conditions as described above. In total, 10 brains were collected per sample and added into microtubes containing 50 µL of PBS and kept in ice during the end of the dissections. Immediately after collection, samples were frozen at – 80°C and stored in the freezer. A total of 10 glioma samples, 12 *UAS*-control samples and 12 *Gal4*-control samples were prepared. For metabolite extraction, the samples were taken out of the freezer and 450 µL of an acetonitrile / water: 50/50 solution were added to the microtubes and sonicated for 5 minutes in an ice bath [58, 63]. The samples were then centrifuged for 10 minutes at 10000 rpm at 5°C. 400 µL of supernatant were collected and transferred to pierced microtubes to allow the acetonitrile to evaporate in a speed-

vac during 30 minutes. The samples were then freeze-dried overnight and the dry products were stored at -80°C.

To prepare the solution-state NMR samples, the dry extracts were taken out of the freezer and solubilized by adding 250 µL of phosphate buffer (PBS 0.1 M, pH 7.4 made in D_2O) also containing Sodium 3-trimethylsilyl [2,2,3,3-d_4] propionate (TSP) for chemical shift referencing. Samples were vortexed and centrifuged 10 minutes and 250 µL were transferred to 3 mm NMR tubes before analysis.

The ^{1}H-NMR measurements were performed on a Bruker 700 MHz Avance III HD spectrometer (Bruker BioSpin, Germany) equipped with a Bruker 5 mm cryoprobe. Solution-state NMR data was acquired using a cpmgpr1D pulse program with water suppression. Each FID was acquired in 32k points for 256 scans and an acquisition time of 26 minutes. 2D homonuclear NMR experiments such as Total Correlation Spectroscopy (TOCSY), Correlation Spectroscopy (COSY) and ^{13}C-HSQC were also recorded on some samples for spectral annotation.

High Resolution Magic Angle Spinning (HR-MAS) analysis

Third instar larvae were dissected in a drop of ice-cold phosphate buffer (pH 7.4 made in D_2O) under the microscope in order to collect their brains and in a maintained cool environment to limit metabolic degradation. Ten to 15 brains and a drop of PBS were transferred into a 4 mm HR-MAS rotors. A total of 15 glioma samples, 9 *UAS*-control samples and 8 *Gal4*-control samples were prepared. Once ready, each sample was analyzed on a Bruker 750 MHz Avance III HD spectrometer (Bruker BioSpin, Germany) equipped with a Bruker 4 mm MAS probe. The sample was kept at 3°C with a rotor spinning frequency of 4 kHz. HR-MAS NMR data was acquired using a spin echo (echo time of 2 rotor periods) with water suppression. Each FID was acquired in 40k points for 1024 scans and an acquisition time of 53 minutes. 2D ^{1}H-^{1}H Total through Bond correlation SpectroscopY (TOBSY) experiments were also performed on several samples for assigning the observed peaks.

2.3 NMR data processing and statistical analysis

Each HR-MAS spectrum was phased and normalized by the number of brains in the sample with Bruker TopSpin 3.5. Each solution-state ^{1}H-NMR spectrum was phased and referenced to TSP resonance. Baseline correction, chemical shift alignment and then 0.01 ppm bucketing of the preprocessed HR-MAS data and solution-state 1H-NMR data were done using the web-based NMR Processing tool NMRProcFlow [64].

Statistical analyses were carried out on Workflow4Metabolomics [65] from both solution-state ^{1}H-NMR and HR-MAS data sets. First, all spectra were normalized using the total intensity method. Then, multivariate analyses were performed on each set of normalized data: i) Principal Component Analysis (PCA) was performed to get an unsupervised overview of the grouping between samples and spot any potential outlier; ii) Orthogonal Partial Least Square Discriminant Analysis (OPLS-DA) [66] were performed using either glioma or control as discriminant conditions to certify that a prediction model could be built based on the experimental data. A seven-fold cross-validation method was used to prevent over-fitting and to assess the significance of the model by giving the Q2 value. A permutation testing, using 100 permutations, further validates the model. Only variables with a Variable Importance in Projection (VIP) calculated from the OPLS-DA models above 1 were kept; *t*-tests were then performed on the filtered data. Differences between groups were considered significant if false discovery rate (fdr) corrected p-values were under the 0.05 threshold. The OPLS-DA multivariate analyses permitted to select the variables differentiating the glioma samples from the controls and univariate analyses (*t*-test) were done to confirm the significance of the variables.

2.4 Metabolite identification and pathway analysis

For the sake of metabolites identification, a concentrated sample prepared with 100 glioma brain extracts was analyzed by 2D solution NMR experiments (TOCSY, COSY and ^{13}C-HSQC).

For both the solution-state NMR and HRMAS data sets, buckets involved in the differentiation between glioma and controls were identified. Then the corresponding signals were assigned to

metabolites using online databases such as the Human Metabolome Database (HMDB) and the BioMagResBank (BMRB) and the 2D NMR experiments [67, 68] leading to list of discriminant metabolites between control and glioma samples.

The list of discriminant metabolites was used as entry into the Pathway Analysis module of MetaboAnalyst [69] to identify the impacted pathways.

2.5 Biomarker Analysis

For identifying potential biomarkers and evaluating their performance, one or two buckets of each discriminant metabolite (with the exception of benzoate) were extracted from data matrices (for both solution-state NMR and HR-MAS). The ability of each metabolite to separate glioma from control samples was tested with receiver operating characteristic (ROC curves) on the web server MetaboAnalyst [69]. ROC curve is probability curve representing specificity (false positive rate) versus sensitivity (true positive rate). AUC (Area under ROC curve) measures the degree of separability of glioma from control samples. It tells how much the model is capable of distinguishing between the two batches of samples. Then, the separation capacity of several groups of randomly selected metabolites was investigated. Classical univariate ROC curve analyses as well as multivariate ROC curve analyses based on PLS-DA, SVM or Random Forests algorithms have been carried out. Finally, four biomarkers were manually selected to evaluate and validate their performance to correctly sort the samples by data mining with linear SVM algorithm (support vector machine algorithm).

3. Results

3.1 Glioma model

A *Drosophila* genetic model for glioma has been successfully developed by Read et al. [37] by co-activation of constitutive forms of EGFR ($dEGFR^{\lambda}$) and PI3K ($dp110^{CAAX}$) specifically in glial cells using the *Gal4- repo* driver which express Gal4 specifically in glial cells at all developmental stages. When we

crossed *UAS-dp110^{CAAX};UAS-GFP;UAS-EGFR$^{\lambda}$* virgins with *UAS-GFP; repo-Gal4/TMTbSb* males, we observed enlarged and deformed brains in *UAS-dp110^{CAAX};UAS-GFP;UAS-EGFR$^{\lambda}$;repo-Gal4* larvae confirming abnormal glial cell proliferation induced by the transgenes (**Figure 1**) as described by Read et al. [37]. No tumors were detected elsewhere in the larvae. The two control groups (*Gal4*-controls and *UAS*-controls) exhibited normal brains.

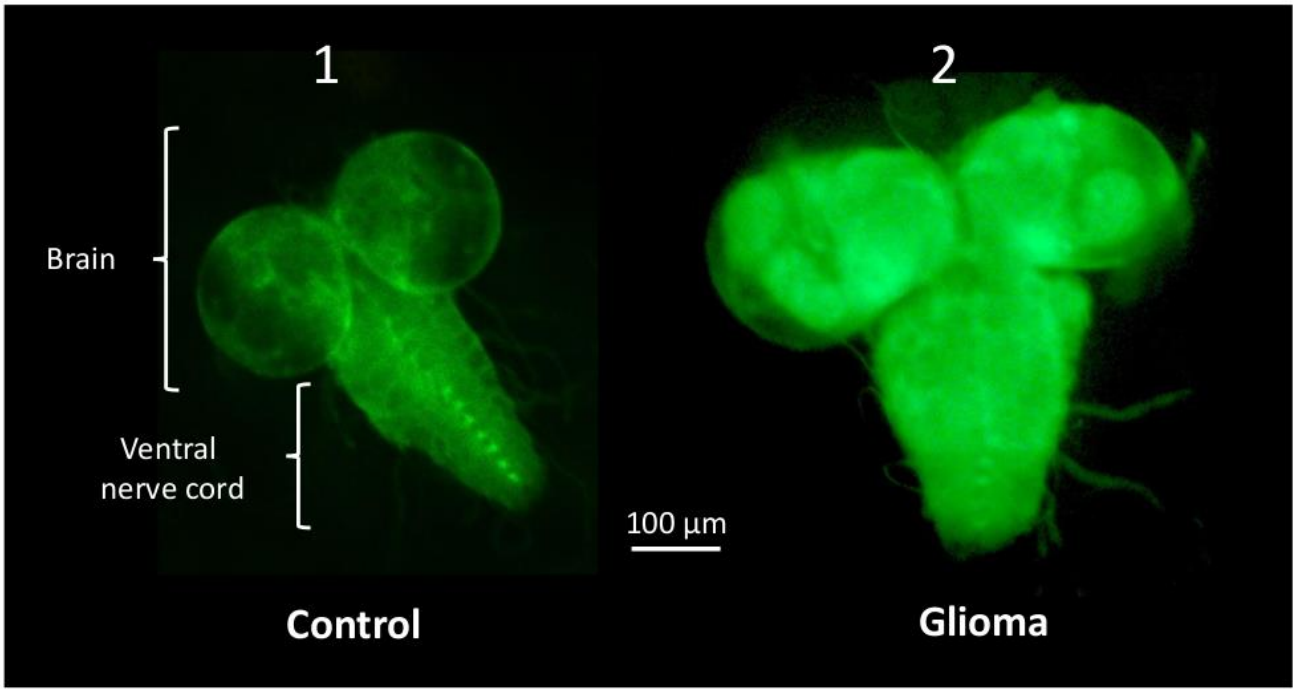

Figure 1. Fluorescence microscopy images of *Drosophila melanogaster* 3rd instar larval brains. Green Fluorescent Protein (GFP) is expressed in glial cells. (1): control *w^{1118}; UAS-GFP; repo-Gal4;* (2): Glioma model *UAS-dp110^{CAAX}; UAS-GFP; UAS-EGFR$^{\lambda}$; repo-Gal4.* The glioma model brain is larger and deformed revealing abnormal glial cell proliferation.

3.2 NMR results

Well resolved ^{1}H spectra were obtained from HR-MAS and solution-state NMR with small amount of material. Up to 47 metabolites could be identified with solution-state NMR and about 20 with HR-MAS (**Figure 2**). Because of the solvent chosen for extraction, lipids were not present in the solution-state NMR samples, which brought the advantage of revealing weak (such as the lactate one at 1.33 ppm) that

would normally be hidden under the intense fatty acids peaks. Hence, HR-MAS data was used to determine lipids' significance in the model.

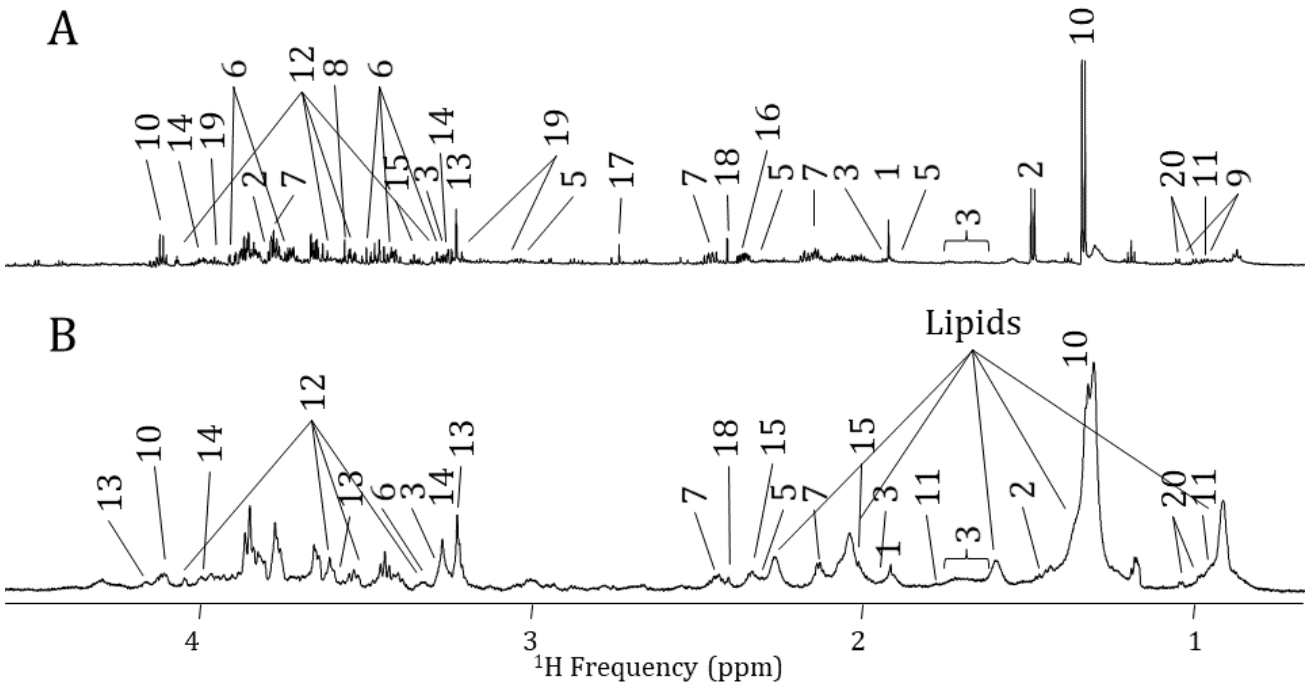

Figure 2. Annotated ^{1}H NMR spectra of glioma samples between 0.70 and 4.5 ppm: (A) 700 MHz solution-state NMR spectrum of 3rd instar larval brain extracts (n=10) and (B) 750 MHz HR-MAS spectrum of fresh 3rd instar larval brains samples (n=10-15). The 20 discrimant metabolites reported in Table 1 and Table S2 are annotated. 1: Acetate 2: Alanine 3: Arginine 4: Benzoate (non visible in this frequency range) 5: GABA 6: Glucose 7: Glutamine 8: Glycine 9: Isoleucine 10: Lactate 11: Leucine 12: Myo-inositol (MI) 13: Phosphocholine (PC) 14: Phosphoethanolamine (PE) 15: Proline 16: Pyruvate 17: Sarcosine 18: Succinate 19: Tyrosine 20: Valine. Note that the lactate peak at 1.33 ppm is annotated for HR-MAS spectra even if not found discriminant. Same for PC on solution-state NMR spectra at 3.21 ppm. Superposition of spectra from control and glioma samples clearly show changes in the level of several metabolites (Figure S1).

3.3 Statistical analysis, metabolite identification and pathway analysis

First, unsupervised multivariate analyses PCA were performed with different components (component 1 as abscissa and component 2 as ordinate). On the solution-state NMR data set (**Figure 3 top left**) PCA analyses showed a clear separation between the glioma group and the controls indicating

differences in metabolite composition. The two control groups were very similar. For the HR-MAS data set, the separation between the glioma group and the controls is less clear (**Figure 3 bottom left**). However, as in the first case, the two control groups were also quite similar. Thus we decided to merge control groups as one for further statistical analysis. Orthogonal Partial Least Squares discriminant analysis (OPLS-DA) were then performed. OPLS, that is a supervised multivariate analysis, enables to separately model the variation correlated (predictive) to the factor of interest and the uncorrelated (orthogonal) variation. OPLS-DA were performed using either glioma or controls as discriminant conditions to certify that a prediction model could be built based on the data (**Figure 3 right**). Very good Q2Y values ($0 \leq Q2Y \leq 1$) of 0.92 for the solution-state NMR data and 0.86 for the HR-MAS data were obtained assessing the quality of the predictions. Thus, with each set of data, the model built by the OPLS-DA clearly shows that glioma samples and controls have different metabolic fingerprints and this model allows to successfully predict the nature of the samples.

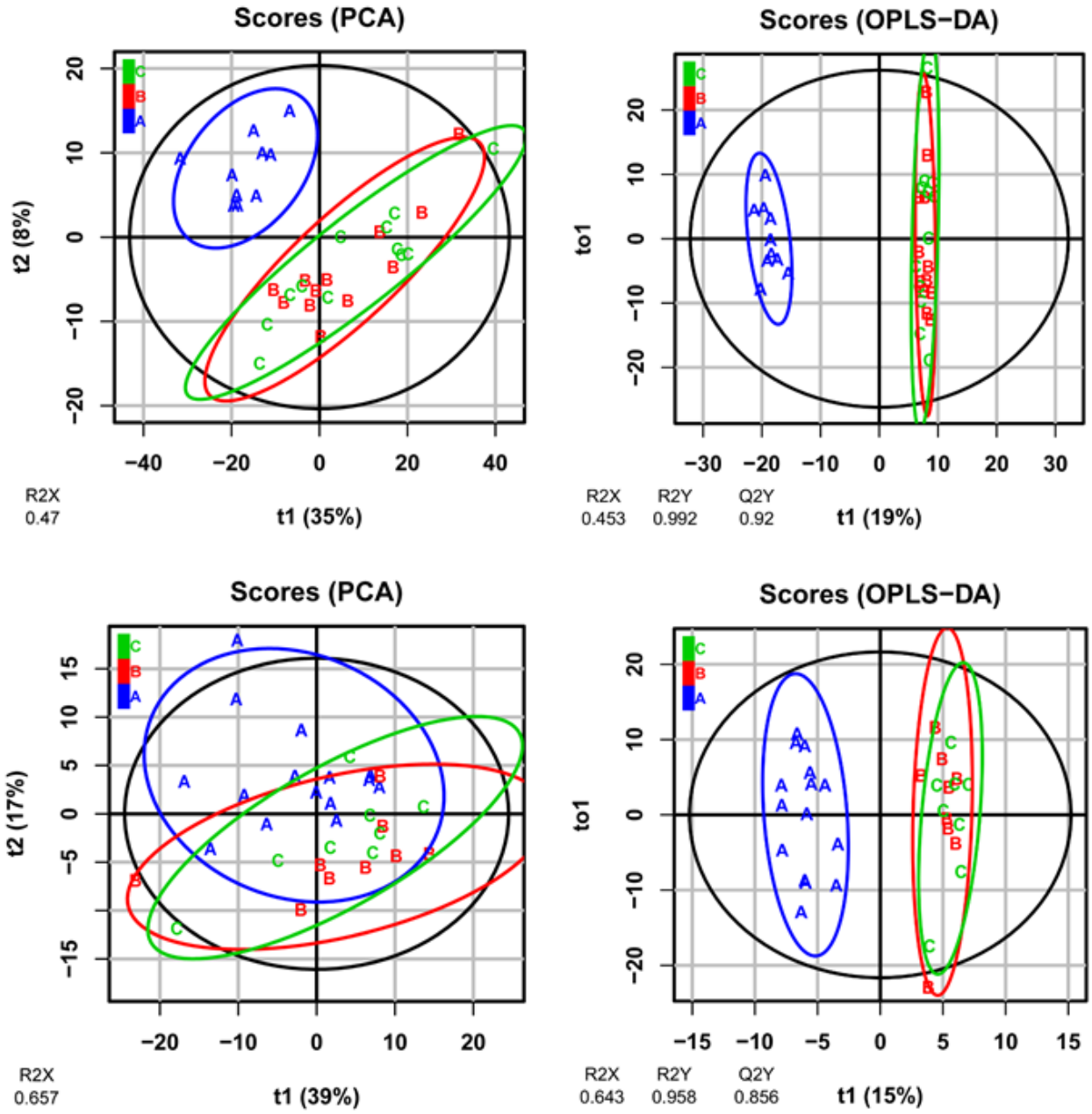

Figure 3. Multivariate analyses score plots. **Top**: Solution-state NMR results. **Bottom**: HR-MAS results. **Left**: Unsupervised multivariate analysis PCA. **Right**: Supervised multivariate analysis OPLS-DA. **Blue:** glioma model samples. **Red:** *w*^{1118}*; UAS-dp110*^{CAAX}*; UAS-EGFR*$^{\lambda}$ controls. **Green:** *w*^{1118}*; UAS-GFP; repo-Gal4* controls. R2X is the percentage of the data matrix X explained by the model, R2Y is the percentage of the response Y explained by the model, Q2Y is the quality of the prediction.

Finally, the data matrixes were filtered to retain the variables having a VIP above 1 and *t*-tests were performed to obtain the buckets significantly different between glioma and control samples with a p-value of less than 0.05. The metabolites related to these buckets were identified. In total, 20 metabolites were identified, 14 with HR-MAS and 19 with the solution-state NMR data. The 20 metabolites were: acetate, alanine, arginine, benzoate, γ-aminobutyrate (GABA), glucose, glutamine, glycine, isoleucine, lactate, leucine, myo-inositol, phosphocholine (PC), phosphoethanolamine (PE), proline, pyruvate, sarcosine, succinate, tyrosine, and valine. Among them, 13 metabolites were common to both methods (**Figure 4**). Overall all the biomarkers found with HR-MAS were also extracted with the solution-state NMR except for PC. The average relative variations of biomaker concentrations between control and glioma samples were determined from integrated intenties of well-resolved peaks characteristic of each metabolites in solution-state and HR-MAS spectra (**Table 1**). With the exception of myo-inositol which shows a huge increase (fold change >3) which can be explained by the glial cell proliferation, the other metabolites show a more modest fold change. Most of the metabolites identified here in *Drosophila* larvae brains have already been reported in studies using various human sample sources (Human GBM cultured cells, biopsies, cerebrospinal fluid, plasma, serum) and different techniques (^{1}HNMR spectroscopy, HR-MAS, *in vivo* imaging, GC/MS) (**Table 1**). Glucose has not been identified in humans, but its presence can be expected as cancer cells, and more specifically GBM cells increase glucose uptake.

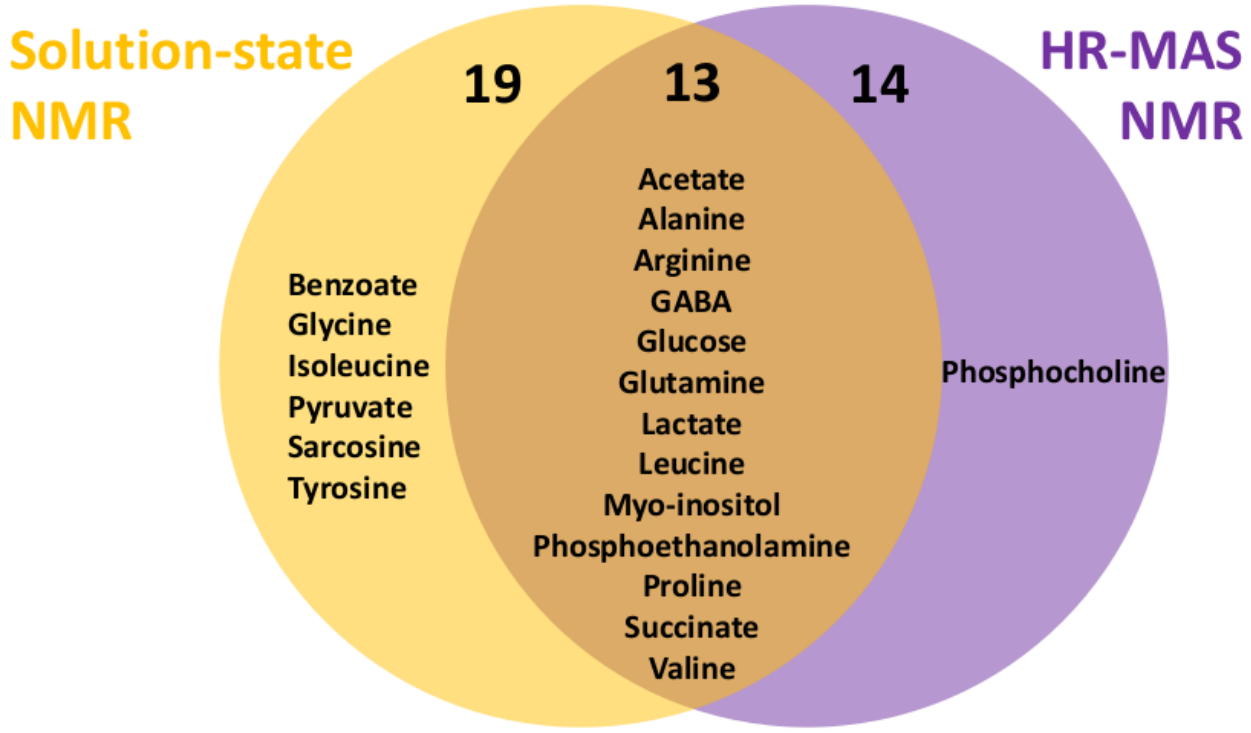

Figure 4. Venn diagram of the identified metabolites for the glioma model developed in *Drosophila melanogaster*. In total, 14 were found discriminant with HR-MAS analysis and 19 with solution-state NMR. Thirteen of these biomarkers were identified with both methods.

The metabolic pathways mainly impacted in glioma samples (**Table 1**) correspond to energetic pathways (glycolysis, TCA cycle) and anabolic pathways (amino-acid metabolism, TCA cycle).

	Discriminant metabolites	NMR p-val	NMR G-C/C	HR-MAS p-val	HR-MAS G-C/C	Metabolites previously detected in Human	Metabolic Pathways
1	Acetate	** 1.92 ppm	↗ 31%	*** 1.92 ppm	↗ 35%	Glioma cell lines grade II vs grade IV [70] (Shao, 2014)	Glycolysis, gluconeogenesis - Pyruvate metabolism
2	Alanine	*** 1.49 ppm	↗ 73%	* 1.44 ppm	↗ 28%	Cerebrospinal fluid samples glioma vs healthy [71] (Ballester, 2018)	Alanine aspartate and glutamate metabolism
3	Arginine	*** 3.24 ppm	↗ 66%	**	↗ 34%	Plasma samples of low grade vs high grade [72] (Zhao, 2016)	Arginine and proline metabolism
4	Benzoate	*** 7.49 ppm	↘ -22%			Serum samples from GBM patients vs healthy [73-75] (Huang, 2017; Bjorkblom, 2016; Chen, 2016)	Benzoate metabolism

5	GABA	** 2.30 ppm	↘ -22%	** 2.30 ppm	↘ -8%	GBM cells and GBM tissues vs normal human astrocytes [76] (Palanichamy, 2016)	Alanine aspartate and glutamate metabolism - Arginine and proline metabolism
6	Glucose	*** 3.26 ppm	↗ 134%	** 3.24 ppm	↗ 34%		Glycolysis, gluconeogenesis
7	Glutamine	*** 2.46 ppm	↗ 48%	* 2.14 ppm	↗ 21%	Glioma cell lines (grade IV vs. II) [70] (Shao, 2014)	Alanine aspartate and glutamate metabolism - Purine and pyrimidine metabolism - Arginine biosynthesis
8	Glycine	*** 3.57 ppm	↗ 43%			Cerebrospinal fluid samples of glioma vs healthy [71] (Ballester, 2018)	Glycine, serine and threonine metabolism - Carbon metabolism
9	Isoleucine	*** 1.46 ppm	↘ -61%			Plasma samples glioma vs healthy [77] (Kelimu, 2016)	Valine, leucine and isoleucine degradation
10	Lactate	*** 4.13 ppm	↗ 43%	* 4.12 ppm	↗ 16%	Plasma sample high grade vs low grade glioma [72] (Zhao, 2016)	Glycolysis, gluconeogenesis - Pyruvate metabolism
11	Leucine	** 0.97 ppm	↗ 28%	** 0.94 ppm	↗ 18%	Glioma cell lines (grade IV vs. II) 70 (Shao, 2014)	Valine, leucine and isoleucine degradation
12	Myoinositol	*** 3.54 ppm	↗ 282%	*** 3.52 ppm	↗ 229%	HGG vs PCNSL [78] (Nagashima, 2018)	Inositol phosphate metabolism
13	PC			** 3.21 ppm	↗ 21%	Brain biopsies of GBM vs. grade II astrocytomas [79] (Wright, 2010)	Glycerophospholipid metabolism
14	PE	** 4.00 ppm	↗ 62%	** 3.99 ppm	↗ 47%	Brain biopsies of GBM vs. grade II astrocytomas [79] (Wright, 2010)	Glycerophospholipid metabolism
15	Proline	** 3.32 ppm	↘ -59%	** 2.06 ppm	↘ -27%	Brain biopsies of HGOs vs. LGOs [80] (Erb, 2008)	Arginine and proline metabolism
16	Pyruvate	*** 2.38 ppm	↗ 81%			Plasma samples glioma vs healthy [77] (Kelimu, 2016)	Glycolysis, gluconeogenesis and pyruvate metabolism
17	Sarcosine	*** 2.76 ppm	↗ 83%			Plasma samples mutant IDH glioma vs wild type IDH glioma [72] (Zhao, 2016)	Glycine, serine and threonine metabolism - Choline metabolism
18	Succinate	*** 2.41 ppm	↗ 32%	* 2.41 ppm	↗ 36%	Plasma samples mutant IDH glioma vs wild type IDH glioma[71, 81, 82] (Ballester, 2018; Nakamizo, 2013; Kalinina, 2016)	Citrate cycle (TCA)
19	Tyrosine	*** 7.21 ppm	↗ 74%			Glioma cell lines (grade IV vs. II) 70 (Shao, 2014)	Phenylalanine and tyrosine metabolism
20	Valine	* 1.05 ppm	↗ 40%	* 1.03 ppm	↗ 44%	Glioma cell lines (grade IV vs. II) [80] (Erb, 2008)	Valine, leucine and isoleucine degradation

Table 1. Identified metabolites discriminating glioma brains from control samples analyzed by solution-state NMR and HR-MAS. References associated with human gliomas. Impacted metabolic pathways. The resulting metabolites were identified by first filtering the buckets from the data matrices given by the OPLS-DA with a VIP threshold of 1 and then by performing a *t*-test on the remaining variables with a p-value threshold of 0, 05. Metabolite bucket selected for p-value calculations and the ratio of the difference in mean between glioma and

control samples to the mean of the control samples (G-C/C). * p-value < 0.05, ** p-value < 0.01, *** p-value < 0.001. ↗: increased relative levels and ↘: decreased relative levels in the glioma samples compared to the controls. **Abbreviations :** GBM: glioblastoma; HGG: High Grade Glioma; PCNSL: primary central nervous system lymphoma; HGO: High Grade oligodendrioma; LGO: low grade oligodendrioma; IDH: isocitrate dehydrogenase

	Discriminant	NMR		HR-MAS		Metabolites previously detected in Human	Metabolic Pathways
	metabolites	Chemical shift	Fold change		Fold change		
1	Acetate	** 1.92 ppm	1.31	***	1.35	Glioma cell lines grade II vs grade IV [70] (Shao, 2014)	Glycolysis, gluconeogenesis Pyruvate metabolism
2	Alanine	*** 1.49 ppm	1.73	*	1.28	Cerebrospinal fluid samples glioma vs healthy [71] (Ballester, 2018)	Alanine aspartate and glutam metabolism
3	Arginine	*** 3.24 ppm	1.66	**	1.34	Plasma samples of low grade vs high grade [72] (Zhao, 2016)	Arginine and proline metaboli
4	Benzoate	*** 7.49 ppm	0.75			Serum samples from GBM patients vs healthy [73-75] (Huang, 2017; Bjorkblom, 2016; Chen, 2016)	Benzoate metabolism
5	GABA	** 2.30 ppm	0.78	**	0.92	GBM cells and GBM tissues vs normal human astrocytes [76] (Palanichamy, 2016)	Alanine aspartate and glutam metabolism - Arginine and pro metabolism
6	Glucose	*** 3.26 ppm	2.34	**	1.34		Glycolysis, gluconeogenesis
7	Glutamine	*** 2.46 ppm	1.48	* 2.14 ppm	1.21	Glioma cell lines (grade IV vs. II) [70] (Shao, 2014)	Alanine aspartate and glutam metabolism - Purine and pyrimi metabolism - Arginine biosynth
8	Glycine	*** 3.57 ppm	1.43			Cerebrospinal fluid samples of glioma vs healthy [71] (Ballester, 2018)	Glycine, serine and threonin metabolism - Carbon metabol
9	Isoleucine	*** 1.46 ppm	0.39			Plasma samples glioma vs healthy [77] (Kelimu, 2016)	Valine, leucine and isoleucin degradation
10	Lactate	*** 4.13 ppm	1.43	*	1.16	Plasma sample high grade vs low grade glioma [72] (Zhao, 2016)	Glycolysis, gluconeogenesis Pyruvate metabolism
11	Leucine	** 0.97 ppm	1.28	**	1.18	Glioma cell lines (grade IV vs. II) 70 (Shao, 2014)	Valine, leucine and isoleucin degradation
12	Myoinositol	*** 3.54 ppm	3.82	***	3.29	HGG vs PCNSL [78] (Nagashima, 2018)	Inositol phosphate metabolis
13	PC			**			Glycerophospholipid metaboli

				3.21 ppm	1.21	Brain biopsies of GBM vs. grade II astrocytomas [79] (Wright, 2010)	
14	PE	**		**		Brain biopsies of GBM vs. grade II astrocytomas [79] (Wright, 2010)	Glycerophospholipid metaboli
		4.00 ppm	1.62		1.47		
15	Proline	**		**		Brain biopsies of HGOs vs. LGOs [80] (Erb, 2008)	Arginine and proline metaboli
		3.32 ppm	0.41	2.06 ppm	0.73		
16	Pyruvate	***				Plasma samples glioma vs healthy [77] (Kelimu, 2016)	Glycolysis, gluconeogenesis a pyruvate metabolism
		2.38 ppm	1.81				
17	Sarcosine	***				Plasma samples mutant IDH glioma vs wild type IDH glioma [72] (Zhao, 2016)	Glycine, serine and threonin metabolism - Choline metabol
		2.76 ppm	1.83				
18	Succinate	***		*		Plasma samples mutant IDH glioma vs wild type IDH glioma[71, 81, 82] (Ballester, 2018; Nakamizo, 2013; Kalinina, 2016)	Citrate cycle (TCA)
		2.41 ppm	1.32		1.36		
19	Tyrosine	***				Glioma cell lines (grade IV vs. II) 70 (Shao, 2014)	Phenylalanine and tyrosine metabolism
		7.21 ppm	1.74				
20	Valine	*		*		Glioma cell lines (grade IV vs. II) [80] (Erb, 2008)	Valine, leucine and isoleucin degradation
		1.05 ppm	1.40		1.44		

Table 2. Identified metabolites discriminating glioma brains from control samples analyzed by solution-state NMR and HR-MAS. References associated with human gliomas. Impacted metabolic pathways. The resulting metabolites were identified by first filtering the buckets from the data matrices given by the OPLS-DA with a VIP threshold of 1 and then by performing a *t*-test on the remaining variables with a p-value threshold of 0, 05. Metabolite bucket selected for p-value and ratio of the mean of glioma samples to the mean of control samples calculations (G/C). * p-value < 0.05, ** p-value < 0.01, *** p-value < 0.001. ↗: increased relative levels and ↘: decreased relative levels in the glioma samples compared to the controls. **Abbreviations :** GBM: glioblastoma; HGG: High Grade Glioma; PCNSL: primary central nervous system lymphoma; HGO: High Grade oligodendrioma; LGO: low grade oligodendrioma; IDH: isocitrate dehydrogenase

3.4 Biomarker Analysis

To evaluate the ability of each metabolite to discriminate glioma samples from controls, metabolites were analyzed individually by the area under the curve ($0 \leq AUC \leq 1$) in the receiver operator characteristics (ROC) curve and *t*-tests values presented in **Table S2**. For the solution-state NMR, individual metabolites were found to have a significant AUC between 1.0 (for glucose, myo-inositol, sarcosine and glycine) and 0.82 (for acetate). For HR-MAS, the AUC values of the individual metabolites range from 0.98 (for myo-inositol) to 0.75 (for lactate).

The multivariate ROC curves obtained with solution-state NMR data, show that glucose (AUC= 1, *t*-test value= $6.09E^{-17}$), myo-Inositol (AUC= 1, *t*-test value= $1.24E^{-16}$), sarcosine (AUC= 1, *t*-test value= $5.94E^{-11}$), and glycine (AUC= 1, *t*-test value= $1.64E^{-10}$) reached very good power in discriminating glioma samples from controls, all samples being classified correctly with each of the four metabolites (**Figure 5**).

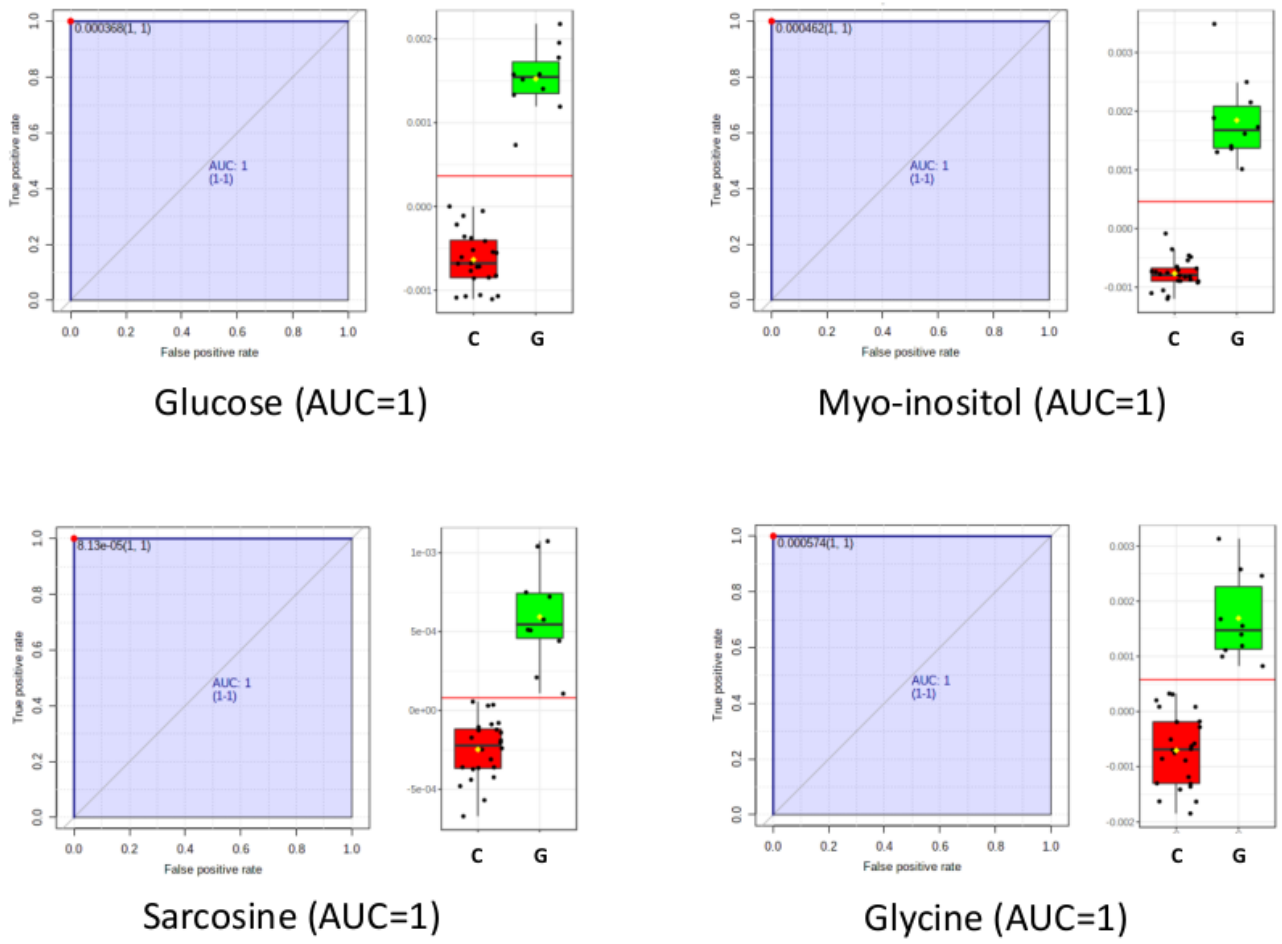

Figure 5. Solution-state NMR biomarker analysis – ROC curves for individual biomarker and boxplots of the four most discriminant metabolites between glioma samples (G, in green) and controls (C, in red). AUC: area under the ROC curve.

Likewise, the multivariate ROC curves of four most discriminant metabolites, obtained with HR-MAS data, were proline (AUC= 0.98, *t*-test value= $3.68E^{-10}$), myo-inositol (AUC= 0.97, *t*-test value= $4.91E^{-09}$), acetate (AUC= 0.94, *t*-test value= $8.87E^{-06}$) and glucose (AUC= 0.90, *t*-test value= $6.73E^{-05}$). These metabolites reached very good power in discriminating glioma samples from controls (**Figure 6**).

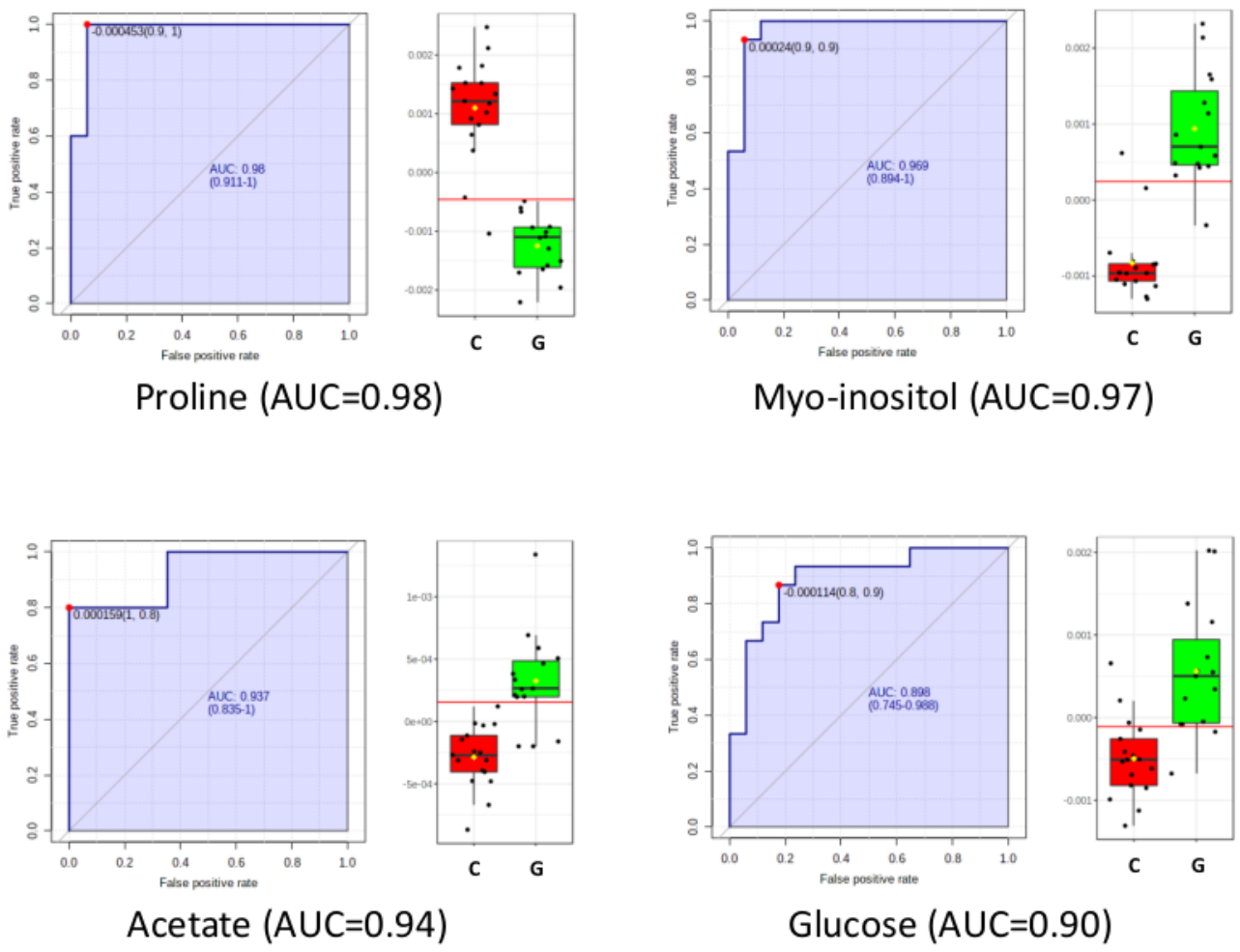

Figure 6. HR-MAS biomarker analysis – ROC curves for individual biomarker and boxplots of the four most discriminant metabolites between glioma samples (G, in green) and controls (C, in red). AUC: area under the ROC curve.

After testing the ability of individual metabolites to separate glioma samples from controls, the separation capacity of selected groups of metabolites was investigated. For solution-state NMR, a group of 4 metabolites (glucose, myo-inositol, sarcosine and glycine) correctly discriminates all 10 glioma samples from the 24 control samples (**Figure 1S**). For HR-MAS, a group of 4 metabolites (proline, myo-inositol, acetate and glucose) correctly discriminates 30 out of 32 samples. Only one glioma sample and one control sample are incorrectly classified (**Figure 2S**).

4. Discussion

Solution-state ^{1}H NMR and ^{1}H HR-MAS are complementary methods which allow to discriminate between normal and diseased flies.

In this study, we identified metabolite biomarkers in a transgenic model of glioblastoma (GBM) in *Drosophila melanogaster.* We used two complementary NMR spectroscopy approaches: i) solution-state ^{1}H NMR commonly used for biomarker discovery and known for producing good and highly reproducible results and ii) ^{1}H HR-MAS NMR, for which such biomarkers identifications in metabolomics is less common but which fully reflects *in vivo* mechanisms. HR-MAS spectroscopy was directly performed on dissected brains without preparation (*ex-vivo*) and extraction bias, providing a complementary and more accurate view of the biochemical mechanisms. As expected, more metabolites (19 versus 14) were identified with solution-state NMR because of the higher resolution and sensitivity. However some metabolites such as lipids or phosphocholine could be detected using HR-MAS but not from the solution-state NMR analysis because of the chosen extraction method. Indeed, the extraction procedure partially removes choline-containing compounds from the tissue that may have close association with cell membranes. Nevertheless 13 metabolites were common to both methods: acetate, alanine, arginine, GABA, glucose, glutamine, lactate, leucine, myo-inositol, phospho-ethanolamine, proline, succinate and valine. Among metabolites not detected as discriminant in HR-MAS analysis, most displayed resonances which overlap with others. The lower resolution of HR-MAS does not allow to unambiguously discern them. This is the case for example of glycine (a single resonance at 3.56 ppm), which is very difficult to separate from myo-inositol (resonances at 3.27, 3.52, 3.61 and 4.05 ppm).

Prediction models were built with results obtained from the two methods, solution-state ^{1}H NMR and ^{1}H HR-MAS NMR, allowing to discriminate control and diseased flies, as demonstrated by the OPLS-DA and ROC curves analysis. Evaluation of biomarkers by ROC analysis showed that all metabolites had a strong discriminating power since their AUC values were all above 0.82 for the solution-state NMR and all above 0.75 for the HR-MAS. In the case of solution-state NMR, with each of the four most discriminant metabolites (glucose, myo-inositol, sarcosine and glycine) or a combination of these four metabolites,

models correctly sorting 100% of the samples could be established. In the case of HR-MAS, the model with the four most discriminant metabolites (proline, myo-inositol, acetate and glucose) correctly sorts 30 of the 32 samples (94%).

These results also demonstrate that the two methods allow identification of glioma specific metabolites and consequently to access to the metabolic reprogramation in the glioma *Drosophila* model. Most of the metabolites identified in this study have been already identified in human samples (table 1), indicating the relevance of the *Drosophila* model. These metabolites constitute tools for detection and treatment of gliomas. Some of them could be used for early detection of gliomas. Currently, there are few biomarkers allowing early detection of gliomas. Several studies using multiparametric MRI texture analysis [70], circulating biomarkers [71] or micro RNAs [72] have shown their usefulness as biomarkers for patients with glioma. The model used in our study does not discriminate which of the metabolites are more characteristic of an early glioma. However, it is interesting to note that we have found myo-inositol and glutamine as strong signatures of glioma in *Drosophila*, metabolites proposed by Kallenberg et al. as markers of early neoplastic infiltration [73].

These metabolites highlight metabolic modifications of the tumor essential to its progression and open the way to new therapeutic approaches targeting these metabolic pathways. *Drosophila* is a particularly relevant model for testing the effectiveness of such approaches. Finally, these metabolites may constitute reliable biomarkers with high diagnostic performance that could be used to follow the evolution of glioma during therapeutic treatment studies in *Drosophila.*

Altered metabolism in the Glioma *Drosophila* model

The metabolic properties of cancer cells differ significantly from those of normal cells. In fact, they must be able to capture nutrients in the external medium in a significant way to produce ATP, to synthesize macromolecules (proteins, lipids, nucleic acids) and their precursors, to ensure their proliferation and to tolerate oxidative stress or hypoxia for example. All this requires a reprogramming

of the metabolic pathways. Discriminant metabolites identified in this study highlight altered metabolism of cancer cells. The main metabolic pathways affected in our glioma model are energetic pathways (glycolysis, TCA cycle), amino acids metabolism and glycerophospholipid metabolism (**Table 1**).

Among the metabolites, which have a higher level in glioma, myo-inositol (MI) was the most predominant marker, its significant elevation in the glioma model being detected with the two NMR methods. MI is produced by astrocytes in adult brain and is a marker of astrogliosis [74-76]. Moreover, MI is involved in the activation of protein kinase C, which activates some proteolytic enzymes responsible for cell invasion in glioma, as for example matrix metalloproteases [77-79] and in the synthesis of phosphatidylinositol lipids [80]. MI is also an important osmolyte in the brain which is involved in the regulation of the intracellular osmolality to adapt changes in the extracellular compartment. Several studies have already linked MI levels to glioma malignancy [73, 79, 81]. Increased levels are found in lower grade astrocytomas compared to GBM and control brains which are consistent with higher survival rate in patients [81]. Therefore most aggressive forms of glioma seem to have lower MI pool because its metabolism is upregulated while in low grade astrocytomas MI pathway is less activated resulting in its accumulation [79]. It has also been proposed that the variation in MI concentration may reflect the integrity of the brain blood-barrier which is disrupted in GBMs, leading to modification of the osmotic environment [82]. The increased level of MI suggests that our model would be closer to a low grade astrocytoma or that the brain blood-barrier is not disturbed.

A major modification of the metabolism in cancer cells is the use of aerobic glycolysis to produce ATP (Warburg effect) leading to the production of lactate [24]. We actually found a significant higher relative concentration of lactate and pyruvate in our glioma model which may reflect Warburg effect. Under normal conditions astrocytes already favored the use of glycolysis to produce lactate and alanine that are used to fuel neurons [83, 84]. We can note that in parallel to the increase in lactate we also showed an increase in alanine. We also detected a higher level of glucose and acetate in glioma samples. These two metabolites are bioenergetic substrates used in cancer cells, in particular in gliomas [85]. It has also been shown that activation of the EGFR pathway in gliomas increases the uptake of glucose and also of acetate [32].

Levels of several amino acids displayed different ratios in glioma as compared to the controls (alanine, arginine, glutamine, glycine, isoleucine, leucine, proline, tyrosine and valine). High levels of some these amino acids have already been reported in brain tumors and in extracellular fluids of brain tumors [86]. Cancer cells often display higher expression of transporters and receptors for amino acids [87] and it has been shown that glioma cells also increase their amino acids uptake [22, 28].

Cancer cells need high level of amino acids to support protein synthesis but also to produce energy. Some of amino acids may be used as alternative sources to fuel the TCA cycle. Several studies have shown that mitochondria are altered in GBM and then could compromise the OXPHOS [88, 89]. As the Warburg effect is not efficient in ATP production, GBM cells need to use other nutrients to produce ATP. The important role of glutamine and glutaminolysis is well documented in cancer cells and particularly in GBM [90] but other amino acids may also be catabolized to obtain metabolites which can fuel the TCA cycle, for example valine, leucine or isoleucine may be degraded into succinyl-CoA and then succinate, or tyrosine metabolism may lead to fumarate. In particular it has been shown that GBM cells use in addition to glutamine, acetate and branched-chain amino acids (leucine, valine, isoleucine) to ensure their growth [91] and that the enzymes involved in the biosynthesis of BCAAs (branched chain amino acids) are very important in ensuring tumor proliferation [92, 93]. The use of these amino acids as a source of ATP may explain the increase in succinate we have noted.

The high level of glycine is characteristic of high grade glioma [60, 81]. Previous studies based on the HR-MAS analysis of human biopsies proposed glycine as a biomarker for brain tumors [60]. Higher concentration of glycine have been found in high grade glioma while levels in low grade astrocytomas were unchanged. Recently, a study of Tiwari et al. on glioma patients demonstrated a higher level of glycine in the most aggressive glioma, suggesting a reprogramation of the glycine metabolism [94]. Glycine, a nonessential amino acid, is a neurotransmitter but also participates to the one-carbon cycle metabolic pathway which is involved in synthesis of nucleotides, proteins, lipids and substrates for methylation reactions. Glycine can be synthesized by cell, in the cytosol or in the mitochondria [95]. In the cytosol, glycine is synthesized from glycolysis via the intermediate 3-phosphoglyceraldehyde. In our glioma model, the PI3K/Akt/mTOR pathway known to stimulate glycolysis is constitutively activated which may favor *de*

novo synthesis of glycine. More generally, glycine is a key an amino acid to ensure rapid proliferation of cancer cells and metastasis [96-98]. Locasale et al. [99] demonstrated that in some cancer cells, a large amount of glycolytic carbons are used to synthetize serine and glycine via phosphoglycerate dehydrogenase (PGDH) and that the gene encoding this enzyme is often amplified. Jain et al. [96] have shown that impairing glycine uptake or its biosynthesis in mitochondria prevents the rapid proliferation of cancer cells and that the mortality is greater in breast cancer patients when this pathway is overexpressed. In 2019, Xia et al. [100] reported that in neuroblastoma cells resulting from an aberrant MCYN (member of the MYC family of oncogenic transcription factors) activation, the serine-glycine-one-carbon (SGOC) biosynthetic pathway is activated and that small molecules inhibiting this pathway demonstrate cytotoxicity to cell lines with MCYN activation and xenografts.

Our study also highlighted an increase in phosphocholine (PC) and phosphoethanolamine (PE). PC and PE are involved in biosynthesis of phosphatidylcholine (PtdCho) and phosphatidylethanolamine (PtdE), which are the major constituents of membrane cells, particularly in brain [101]. Elevated levels of PC and PE are a mark of cancer cells [102]. Choline species have been reported to be increased in brain tumors and may reflect increased membrane turnover or cellular density. They have been proposed as marker of gliomas aggressiveness [103, 104]. Increase in PC may also be explained by the activation of the PI3K/Akt/mTOR pathway frequently altered in GBM and involved in our model. This pathway regulates the expression of several genes, in particular the gene that encodes the hypoxia inducible factor 1a (HIF-1α) [105]. HIF-1α controls the expression of choline kinase alpha [106] that catalyzes the synthesis of PC from choline. Increase level of PE has also been reported in biopsy of brain tumors [104, 107, 108]. In addition to its role in metabolism of phospholipids, PC may also be a second messenger involved in cancer growth [109].

In our model, GABA has a lower level in glioma. GABA is a neurotransmitter in the cortex area of the brain. It plays an inhibitor role on synapses [110]. Literature offers conflicting results regarding GABA levels in glioma. Some studies suggest that GABA is less present or not detected in high grade tumors compared to low grade tumors and control brains while others find higher levels of GABA in GBM than in control brains [81, 86, 111]. Other studies describe the metabolic switch of GABA in GBM stem-like cells [112]. Decreased

levels of GABA, associated with increased concentration of its by-products 2-hydroxyglutarate (2-HG) and 4-hydroxybutyrate (GHB), are correlated with a loss of tumorgenicity [112].

Among metabolites displaying an increased level in glioma, two are of particular interest: succinate and lactate. These two metabolites may support carcinogenesis and are considered as oncometabolites [113]. Succinate displays many effects involved in the development of the tumor: it inhibits α-ketoglutarate (αKG)-dependent dioxygenases (αKGDD), a class of enzymes involved in various biological processes. For example, inhibition of prolyl-hydroxylases by succinate, leads to stabilization of hypoxia inducible factor [114]. Succinate may also participates to epigenetic reprograming by inhibition of Ten-Eleven Translocation proteins (TETs) and Histone Lysine Demethylases (KDMs), involved respectively in DNA demethylation and histone demethylation [115-118]. In the same way, lactate is an oncometabolite. It is not only a by-product of glycolysis, it is also a second messenger, acting as a signaling molecule to induce autocrine, paracrine, and endocrine-like effects [119, 120]. The high amounts of lactate secreted by tumor cells leads to an acidification of the tumor microenvironment favoring invasion, metastasis, angiogenesis and suppression of immune response [121]. Lactate may also be involved in epigenetic reprogramation. The work of Bhagat et al. [122] on pancreatic ductal adenocarcinoma, has shown that lactate may indirectly participate to epigenetic reprograming by inducing increased synthesis of alpha-ketoglutarate (αKG) in mesenchymal stem cells surrounding cancer cells. Alpha-ketoglutarate is known to be involved in activation of the demethylase TET Enzyme and Histone Lysine demethylases (JMJD). Recently, Zhang et al. [123] established that lactate can modulate a new histone modification: lysine lactylation. They also showed that this new epigenetic mark may contribute to modulate gene expression. Thus, the mutations we used to perform our glioma model (Pi3K and EGFR gain of function) leads to accumulation of these two oncometabolites which in turn are able to modify the tumor environment and to reprogram gene expression in the tumoral cells to favor its development and aggressiveness. These oncometabolites may constitute key biomarkers useful in diagnosis and prognosis, but they may also be considered as new therapeutic targets. Many studies have been performed to inhibit synthesis of these metabolites. For example, several molecules targeting LDH, which catalyzes the synthesis of lactate from pyruvate have been developed such as oxamate, gossypol, galloflavin, or N-hydroxyindole compounds [124] (for review

see El Hassouni et al. 2020). Gossypol demonstrated a cytotoxic effect on cancer cell lines. It was also used in clinical trials, in particular with patients with malignant glioma [125], but it showed a poor clinical efficacy. Two N-hydroxyindole compounds, NHI-1 and NHI-2, tested in GBM cell lines and glioma stem cells induce apoptosis and cell differentiation [126] but their effect was transient. In addition, a better knowledge of the functions of these oncometabolites could also be useful in finding other therapeutic targets.

3 Conclusion

In this study, glioma model has been successfully induced in *Drosophila melanogaster*, following Read's model [36], by co-activating the Epidermal Growth Factor Receptor (EGFR) and the Phosphatidyl-Inositol-3 Kinase (PI3K) signaling pathways. In total, twenty biomarkers for the glioma *Drosophila* model were identified using NMR based metabolomics. Nineteen discriminant metabolites were detected by solution-state NMR, known as a highly sensitive and highly resolved tool to obtain metabolic fingerprints from brain extracts. Fourteen discriminant metabolites were detected by HR-MAS, allowing to directly observing key metabolites from dissected brains (*ex-vivo*), without further sample preparation. Thirteen metabolites were highlighted by both methods, which shows a very good correlation between them. Among all the identified metabolites, glucose, myo-inositol, sarcosine, glycine, alanine and pyruvate for solution-state NMR and proline, myo-inositol, acetate and glucose for HR-MAS NMR allow to discriminate samples according to their nature with very good performances. This demonstrates that each method by itself is able to identify glioma biomarkers. Nevertheless, a more complete view of the induced disturbances and a better understanding of metabolic pathway impacts are obtained from the combined analysis

Most of identified metabolites were consistent with human oncogenesis and glial cells proliferation. The main metabolic pathways impacted in our glioma model are energetic pathways (glycolysis, TCA cycle), amino acids metabolism and glycerophospholipid metabolism. This study consolidates the interest of *Drosophila melanogaster* in studying and modelling glioma and opens the possibility of deciphering the

biochemical mechanisms disturbed in these tumors. The identified biomarkers provide means to rebalance specific pathways through targeted metabolic therapy, and to study the effects of pharmacological treatments using *Drosophila melanogaster* as a model organism.

Acknowledgments

We thank Hervé Meudal for the upkeep of the NMR spectrometers and Nadège Hervouet for the maintenance of the flies.

Funding Sources

This work was supported by grants from la Région Centre-Val de Loire (LINGO Project), La Ligue contre le Cancer (Loiret and Sarthe commitees) and the IR-RMN-THC Fr3050 CNRS.

Supporting Information

Figure 1S : Comparison of the mean spectra of control and glioma samples in solution-state NMR and HR-MAS.

Table S1 : Solution-state 1H NMR and 1H HR-MAS signals of the identified metabolites discriminating glioma brains from control samples and the impacted metabolic pathways.

Table S2 : Performance measurement of the characteristic bucket(s) of each metabolite.

Figure 2S : Biomarker analysis on a group of four selected metabolites (glucose, myo-inositol, sarcosine and glycine) for the solution-state NMR.

Figure 3S : Biomarker analysis on a group of four selected metabolites (proline, myo-inositol, acetate and glucose) for the HR-MAS.

References

1. Maher, E. A.; Furnari, F. B.; Bachoo, R. M.; Rowitch, D. H.; Louis, D. M.; Cavenee, W. K.; DePinho, R. A., Malignant glioma: genetics and biology of a grave matter. *Genes & Development* **2001,** *15* (11), 1311-1333.
2. Louis, D. N.; Ohgaki, H.; Wiestler, O. D.; Cavenee, W. K.; Burger, P. C.; Jouvet, A.; Scheithauer, B. W.; Kleihues, P., The 2007 WHO classification of tumours of the central nervous system. *Acta Neuropathologica* **2007,** *114* (2), 97-109.
3. Louis, D. N.; Perry, A.; Reifenberger, G.; von Deimling, A.; Figarella-Branger, D.; Cavenee, W. K.; Ohgaki, H.; Wiestler, O. D.; Kleihues, P.; Ellison, D. W., The 2016 World Health Organization Classification of Tumors of the Central Nervous System: a summary. *Acta Neuropathologica* **2016,** *131* (6), 803-820.
4. Ohgaki, H.; Kleihues, P., Population-based studies on incidence, survival rates, and genetic alterations in astrocytic and oligodendroglial gliomas. *Journal of neuropathology and experimental neurology* **2005,** *64* (6), 479-489.
5. Nagane, M.; Coufal, F.; Lin, H.; Bogler, O.; Cavenee, W. K.; Huang, H. J. S., A common mutant epidermal growth factor receptor confers enhanced tumorigenicity on human glioblastoma cells by increasing proliferation and reducing apoptosis. *Cancer Research* **1996,** *56* (21), 5079-5086.
6. Nagane, M.; Levitzki, A.; Gazit, A.; Cavenee, W. K.; Huang, H. J. S., Drug resistance of human glioblastoma cells conferred by a tumor-specific mutant epidermal growth factor receptor through modulation of Bcl-X-L and caspase-3-like proteases. *Proceedings of the National Academy of Sciences of the United States of America* **1998,** *95* (10), 5724-5729.
7. Friedmann-Morvinski, D., Glioblastoma heterogeneity and cancer cell plasticity. *Critical reviews in oncogenesis* **2014,** *19* (5), 327-36.
8. Furnari, F. B.; Fenton, T.; Bachoo, R. M.; Mukasa, A.; Stommel, J. M.; Stegh, A.; Hahn, W. C.; Ligon, K. L.; Louis, D. N.; Brennan, C.; Chin, L.; DePinho, R. A.; Cavenee, W. K., Malignant astrocytic glioma: genetics, biology, and paths to treatment. *Genes & Development* **2007,** *21* (21), 2683-2710.
9. Libermann, T. A.; Nusbaum, H. R.; Razon, N.; Kris, R.; Lax, I.; Soreq, H.; Whittle, N.; Waterfield, M. D.; Ullrich, A.; Schlessinger, J., Amplification, enhanced expression and possible rearrangement of EGF Receptor gene in primary human-brain tumors of glial origin. *Nature* **1985,** *313* (5998), 144-147.
10. Ekstrand, A. J.; James, C. D.; Cavenee, W. K.; Seliger, B.; Pettersson, R. F.; Collins, V. P., Genes for Epidermal Growth-Factor Receptor, transforming growth factor-alpha, and epidermal growth-factor and their expression in human gliomas invivo. *Cancer Research* **1991,** *51* (8), 2164-2172.
11. Wong, A. J.; Ruppert, J. M.; Bigner, S. H.; Grzeschik, C. H.; Humphrey, P. A.; Bigner, D. S.; Vogelstein, B., Structural alterations of the Epidermal Growth-Factor Receptor gene in human gliomas. *Proceedings of the National Academy of Sciences of the United States of America* **1992,** *89* (7), 2965-2969.
12. Sugawa, N.; Ekstrand, A. J.; James, C. D.; Collins, V. P., Identical splicing of aberrant epidermal growth-factor receptor transcripts from amplified rearranged genes in Human glioblastomas. *Proceedings of the National Academy of Sciences of the United States of America* **1990,** *87* (21), 8602-8606.
13. Frederick, L.; Wang, X. Y.; Eley, G.; James, C. D., Diversity and frequency of Epidermal Growth Factor Receptor mutations in human glioblastomas. *Cancer Research* **2000,** *60* (5), 1383-1387.
14. Samuels, Y.; Wang, Z. H.; Bardelli, A.; Silliman, N.; Ptak, J.; Szabo, S.; Yan, H.; Gazdar, A.; Powell, D. M.; Riggins, G. J.; Willson, J. K. V.; Markowitz, S.; Kinzler, K. W.; Vogelstein, B.; Velculescu, V. E., High frequency of mutations of the PIK3CA gene in human cancers. *Science* **2004,** *304* (5670), 554-554.
15. Gallia, G. L.; Rand, V.; Siu, I. M.; Eberhart, C. G.; James, C. D.; Marie, S. K. N.; Oba-Shinjo, S. M.; Carlotti, C. G.; Caballero, O. L.; Simpson, A. J. G.; Brock, M. V.; Massion, P. P.; Carson, B. S., Sr.; Riggins, G. J., PIK3CA gene mutations in pediatric and adult glioblastoma multiforme. *Molecular Cancer Research* **2006,** *4* (10), 709-714.
16. Knobbe, C. B.; Reifenberger, G., Genetic alterations and aberrant expression of genes related to the phosphatidyl-inositol-3 '-kinase/protein kinase B (Akt) signal transduction pathway in glioblastomas. *Brain Pathology* **2003,** *13* (4), 507-518.

17. Kang, S.; Denley, A.; Vanhaesebroeck, B.; Vogt, P. K., Oncogenic transformation induced by the p110 beta, -gamma, and -delta isoforms of class I phosphoinositide 3-kinase. *Proceedings of the National Academy of Sciences of the United States of America* **2006,** *103* (5), 1289-1294.
18. Choe, G.; Horvath, S.; Cloughesy, T. F.; Crosby, K.; Seligson, D.; Palotie, A.; Inge, L.; Smith, B. L.; Sawyers, C. L.; Mischel, P. S., Analysis of the phosphatidylinositol 3 '-kinase signaling pathway in glioblastoma patients in Vivo. *Cancer Research* **2003,** *63* (11), 2742-2746.
19. Cloughesy, T. F.; Yoshimoto, K.; Nghiemphu, P.; Brown, K.; Dang, J.; Zhu, S.; Hsueh, T.; Chen, Y.; Wang, W.; Youngkin, D.; Liau, L.; Martin, N.; Becker, D.; Bergsneider, M.; Lai, A.; Green, R.; Oglesby, T.; Koleto, M.; Trent, J.; Horvath, S.; Mischel, P. S.; Mellinghoff, I. K.; Sawyers, C. L., Antitumor activity of rapamycin in a phase I trial for patients with recurrent PTEN-Deficient glioblastoma. *PLOS Medicine* **2008,** *5* (1), 139-151.
20. Azuaje, F.; Tiemann, K.; Niclou, S. P., Therapeutic control and resistance of the EGFR-driven signaling network in glioblastoma. *Cell Communication and Signaling* **2015,** *13*, 23.
21. DeBerardinis, R. J.; Chandel, N. S., Fundamentals of cancer metabolism. *Science Advances* **2016,** *2* (5), e1600200.
22. Pavlova, N. N.; Thompson, C. B., The Emerging Hallmarks of Cancer Metabolism. *Cell Metabolism* **2016,** *23* (1), 27-47.
23. Yang, L.; Venneti, S.; Nagrath, D., Glutaminolysis: A Hallmark of Cancer Metabolism. In *Annual Review of Biomedical Engineering*, Yarmush, M. L., Ed. 2017; Vol. 19, pp 163-194.
24. Warburg, O., Origin of cancer cells. *Science* **1956,** *123* (3191), 309-314.
25. Zheng, J., Energy metabolism of cancer: Glycolysis versus oxidative phosphorylation. *Oncology Letters* **2012,** *4* (6), 1151-1157.
26. Nagahashi Marie, S. K.; Oba Shinjo, S. M., Metabolism and Brain Cancer. *Clinics* **2011,** *66*, 33-43.
27. Strickland, M.; Stoll, E. A., Metabolic Reprogramming in Glioma. *Frontiers in Cell and Developmental Biology* **2017,** *5*, 43.
28. Venneti, S.; Thompson, C. B., Metabolic Reprogramming in Brain Tumors. In *Annual Review of Pathology: Mechanisms of Disease*, Abbas, A. K.; Aster, J. C.; Feany, M. B., Eds. 2017; Vol. 12, pp 515-545.
29. Lien, E. C.; Lyssiotis, C. A.; Cantley, L. C., Metabolic Reprogramming by the PI3K-Akt-mTOR Pathway in Cancer. *Recent results in cancer research. Fortschritte der Krebsforschung. Progrès dans les recherches sur le cancer* **2016,** *207*, 39-72.
30. Reitman, Z. J.; Jin, G.; Karoly, E. D.; Spasojevic, I.; Yang, J.; Kinzler, K. W.; He, Y.; Bigner, D. D.; Vogelstein, B.; Yan, H., Profiling the effects of isocitrate dehydrogenase 1 and 2 mutations on the cellular metabolome. *Proceedings of the National Academy of Sciences of the United States of America* **2011,** *108* (8), 3270-3275.
31. Dang, L.; White, D. W.; Gross, S.; Bennett, B. D.; Bittinger, M. A.; Driggers, E. M.; Fantin, V. R.; Jang, H. G.; Jin, S.; Keenan, M. C.; Marks, K. M.; Prins, R. M.; Ward, P. S.; Yen, K. E.; Liau, L. M.; Rabinowitz, J. D.; Cantley, L. C.; Thompson, C. B.; Heiden, M. G. V.; Su, S. M., Cancer-associated IDH1 mutations produce 2-hydroxyglutarate. *Nature* **2009,** *462* (7274), 739–744.
32. Bi, J.; Chowdhry, S.; Wu, S.; Zhang, W.; Masui, K.; Mischel, P. S., Altered cellular metabolism in gliomas - an emerging landscape of actionable co-dependency targets. *Nature Reviews Cancer* **2020,** *20* (1), 57-70.
33. Wang, L.-B.; Karpova, A.; Gritsenko, M. A.; Kyle, J. E.; Cao, S.; Li, Y.; Rykunov, D.; Colaprico, A.; Rothstein, J. H.; Hong, R.; Stathias, V.; Cornwell, M.; Petralia, F.; Wu, Y.; Reva, B.; Krug, K.; Pugliese, P.; Kawaler, E.; Olsen, L. K.; Liang, W.-W.; Song, X.; Dou, Y.; Wendl, M. C.; Caravan, W.; Liu, W.; Zhou, D. C.; Ji, J.; Tsai, C.-F.; Petyuk, V. A.; Moon, J.; Ma, W.; Chu, R. K.; Weitz, K. K.; Moore, R. J.; Monroe, M. E.; Zhao, R.; Yang, X.; Yoo, S.; Krek, A.; Demopoulos, A.; Zhu, H.; Wyczalkowski, M. A.; McMichael, J. F.; Henderson, B. L.; Lindgren, C. M.; Boekweg, H.; Lu, S.; Baral, J.; Yao, L.; Stratton, K. G.; Bramer, L. M.; Zink, E.; Couvillion, S. P.; Bloodsworth, K. J.; Satpathy, S.; Sieh, W.; Boca, S. M.; Schurer, S.; Chen, F.; Wiznerowicz, M.; Ketchum, K. A.; Boja, E. S.; Kinsinger, C. R.; Robles, A. I.; Hiltke, T.; Thiagarajan, M.; Nesvizhskii, A. I.; Zhang, B.; Mani, D. R.; Ceccarelli, M.; Chen, X. S.; Cottingham, S. L.; Li, Q. K.; Kim, A. H.; Fenyo, D.; Ruggles, K. V.; Rodriguez, H.; Mesri, M.; Payne, S. H.; Resnick, A. C.; Wang, P.; Smith, R. D.; Iavarone, A.; Chheda, M. G.; Barnholtz-

Sloan, J. S.; Rodland, K. D.; Liu, T.; Ding, L.; Clinical Proteomic Tumor Anal, C., Proteogenomic and metabolomic characterization of human glioblastoma. *Cancer Cell* **2021,** *39* (4), 509-+.
34. Chien, S.; Reiter, L. T.; Bier, E.; Gribskov, M., Homophila: human disease gene cognates in Drosophila. *Nucleic Acids Research* **2002,** *30* (1), 149-151.
35. Bharucha, K. N., The Epicurean Fly: Using Drosophila Melanogaster to Study Metabolism. *Pediatric Research* **2009,** *65* (2), 132-137.
36. Mirzoyan, Z.; Sollazzo, M.; Allocca, M.; Valenza, A. M.; Grifoni, D.; Bellosta, P., Drosophila melanogaster: A Model Organism to Study Cancer. *Frontiers in Genetics* **2019,** *10*, 51.
37. Read, R. D.; Cavenee, W. K.; Furnari, F. B.; Thomas, J. B., A Drosophila Model for EGFR-Ras and PI3K-Dependent Human Glioma. *PLOS Genetics* **2009,** *5* (2), e1000374.
38. Read, R. D., Drosophila melanogaster as a Model System for Human Brain Cancers. *Glia* **2011,** *59* (9), 1364-1376.
39. Chi, K.-C.; Tsai, W.-C.; Wu, C.-L.; Lin, T.-Y.; Hueng, D.-Y., An Adult Drosophila Glioma Model for Studying Pathometabolic Pathways of Gliomagenesis. *Molecular Neurobiology* **2019,** *56* (6), 4589-4599.
40. Beckonert, O.; Coen, M.; Keun, H. C.; Wang, Y.; Ebbels, T. M. D.; Holmes, E.; Lindon, J. C.; Nicholson, J. K., High-resolution magic-angle-spinning NMR spectroscopy for metabolic profiling of intact tissues. *Nature Protocols* **2010,** *5* (6), 1019-1032.
41. Ratai, E. M.; Pilkenton, S.; Lentz, M. R.; Greco, J. B.; Fuller, R. A.; Kim, J. P.; He, J.; Cheng, L. L.; Gonzalez, R. G., Comparisons of brain metabolites observed by HRMAS H-1 NMR of intact tissue and solution H-1 NMR of tissue extracts in SIV-infected macaques. *NMR in Biomedicine* **2005,** *18* (4), 242-251.
42. Elena-Herrmann, B.; Montellier, E.; Fages, A.; Bruck-Haimson, R.; Moussaieff, A., Multi-platform NMR Study of Pluripotent Stem Cells Unveils Complementary Metabolic Signatures towards Differentiation. *Scientific Reports* **2020,** *10* (1), 1622.
43. Malmendal, A.; Overgaard, J.; Bundy, J. G.; Sorensen, J. G.; Nielsen, N. C.; Loeschcke, V.; Holmstrup, M., Metabolomic profiling of heat stress: hardening and recovery of homeostasis in Drosophila. *American Journal of Physiology-Regulatory Integrative and Comparative Physiology* **2006,** *291* (1), R205-R212.
44. Overgaard, J.; Malmendal, A.; Sorensen, J. G.; Bundy, J. G.; Loeschcke, V.; Nielsen, N. C.; Holmstrup, M., Metabolomic profiling of rapid cold hardening and cold shock in Drosophila melanogaster. *Journal of Insect Physiology* **2007,** *53* (12), 1218-1232.
45. Pedersen, K. S.; Kristensen, T. N.; Loeschcke, V.; Petersen, B. O.; Duus, J. O.; Nielsen, N. C.; Malmendal, A., Metabolomic Signatures of Inbreeding at Benign and Stressful Temperatures in Drosophila melanogaster. *Genetics* **2008,** *180* (2), 1233-1243.
46. Williams, C. M.; Watanabe, M.; Guarracino, M. R.; Ferraro, M. B.; Edison, A. S.; Morgan, T. J.; Boroujerdi, A. F. B.; Hahn, D. A., Cold adaptation shapes the robustness of metabolic networks in Drosophila melanogaster. *Evolution* **2014,** *68* (12), 3505-3523.
47. Gogna, N.; Singh, V. J.; Sheeba, V.; Dorai, K., NMR-based investigation of the Drosophila melanogaster metabolome under the influence of daily cycles of light and temperature. *Molecular Biosystems* **2015,** *11* (12), 3305-3315.
48. Sarup, P.; Petersen, S. M. M.; Nielsen, N. C.; Loeschcke, V.; Malmendal, A., Mild heat treatments induce long-term changes in metabolites associated with energy metabolism in Drosophila melanogaster. *Biogerontology* **2016,** *17* (5-6), 873-882.
49. Schou, M. F.; Kristensen, T. N.; Pedersen, A.; Karlsson, B. G.; Loeschcke, V.; Malmendal, A., Metabolic and functional characterization of effects of developmental temperature in Drosophila melanogaster. *American Journal of Physiology-Regulatory Integrative and Comparative Physiology* **2017,** *312* (2), R211-R222.
50. Malmendal, A.; Sorensen, J. G.; Overgaard, J.; Holmstrup, M.; Nielsen, N. C.; Loeschcke, V., Metabolomic analysis of the selection response of Drosophila melanogaster to environmental stress: are there links to gene expression and phenotypic traits? *Naturwissenschaften* **2013,** *100* (5), 417-427.
51. Coquin, L.; Feala, J. D.; McCulloch, A. D.; Paternostro, G., Metabolomic and flux-balance analysis of age-related decline of hypoxia tolerance in Drosophila muscle tissue. *Molecular Systems Biology* **2008,** *4*.

52. Feala, J. D.; Coquin, L.; McCulloch, A. D.; Paternostro, G., Flexibility in energy metabolism supports hypoxia tolerance in Drosophila flight muscle: metabolomic and computational systems analysis. *Molecular Systems Biology* **2007,** *3*.
53. Feala, J. D.; Coquin, L.; Paternostro, G.; McCulloch, A. D., Integrating metabolomics and phenomics with systems models of cardiac hypoxia. *Progress in Biophysics & Molecular Biology* **2008,** *96* (1-3), 209-225.
54. Feala, J. D.; Coquin, L.; Zhou, D.; Haddad, G. G.; Paternostro, G.; McCulloch, A. D., Metabolism as means for hypoxia adaptation: metabolic profiling and flux balance analysis. *Bmc Systems Biology* **2009,** *3*.
55. Bakalov, V.; Amathieu, R.; Triba, M. N.; Clement, M.-J.; Uribe, L. R.; Le Moyec, L.; Kaynar, A. M., Metabolomics with Nuclear Magnetic Resonance Spectroscopy in a Drosophila melanogaster Model of Surviving Sepsis. *Metabolites* **2016,** *6* (4).
56. Singh, V.; Sharma, R. K.; Athilingam, T.; Sinha, P.; Sinha, N.; Thakur, A. K., NMR Spectroscopy-based Metabolomics of Drosophila Model of Huntington's Disease Suggests Altered Cell Energetics. *Journal of Proteome Research* **2017,** *16* (10), 3863-3872.
57. Bertrand, M.; Decoville, M.; Meudal, H.; Birman, S.; Landon, C., Metabolomic Nuclear Magnetic Resonance Studies at Presymptomatic and Symptomatic Stages of Huntington's Disease on a Drosophila Model. *Journal of Proteome Research* **2020,** *19* (10), 4034-4045.
58. Ott, S.; Vishnivetskaya, A.; Malmendal, A.; Crowther, D. C., Metabolic changes may precede proteostatic dysfunction in a Drosophila model of amyloid beta peptide toxicity. *Neurobiology of Aging* **2016,** *41*, 39-52.
59. Constantinou, C.; Apidianakis, Y.; Psychogios, N.; Righi, V.; Mindrinos, M. N.; Khan, N.; Swartz, H. M.; Szeto, H. H.; Tompkins, R. G.; Rahme, L. G.; Tzika, A. A., In vivo high-resolution magic angle spinning magnetic and electron paramagnetic resonance spectroscopic analysis of mitochondria-targeted peptide in Drosophila melanogaster with trauma-induced thoracic injury. *International Journal of Molecular Medicine* **2016,** *37* (2), 299-308.
60. Righi, V.; Andronesi, O. C.; Mintzopoulos, D.; Black, P. M.; Tzika, A. A., High-resolution magic angle spinning magnetic resonance spectroscopy detects glycine as a biomarker in brain tumors. *International Journal of Oncology* **2010,** *36* (2), 301-306.
61. Righi, V.; Apidianakis, Y.; Psychogios, N.; Rahme, L. G.; Tompkins, R. G.; Tzika, A. A., In vivo high-resolution magic angle spinning proton NMR spectroscopy of Drosophila melanogaster flies as a model system to investigate mitochondrial dysfunction in Drosophila GST2 mutants. *International Journal of Molecular Medicine* **2014,** *34* (1), 327-333.
62. Yon, M.; Decoville, M.; Sarou-Kanian, V.; Fayon, F.; Birman, S., Spatially-resolved metabolic profiling of living Drosophila in neurodegenerative conditions using H-1 magic angle spinning NMR. *Scientific Reports* **2020,** *10* (1).
63. Sarup, P.; Pedersen, S. M. M.; Nielsen, N. C.; Malmendal, A.; Loeschcke, V., The Metabolic Profile of Long-Lived Drosophila melanogaster. *PLOS One* **2012,** *7* (10), e47461.
64. Jacob, D.; Deborde, C.; Lefebvre, M.; Maucourt, M.; Moing, A., NMRProcFlow: a graphical and interactive tool dedicated to 1D spectra processing for NMR- based metabolomics. *Metabolomics* **2017,** *13* (4), 36.
65. Giacomoni, F.; Le Corguille, G.; Monsoor, M.; Landi, M.; Pericard, P.; Petera, M.; Duperier, C.; Tremblay-Franco, M.; Martin, J.-F.; Jacob, D.; Goulitquer, S.; Thevenot, E. A.; Caron, C., Workflow4Metabolomics: a collaborative research infrastructure for computational metabolomics. *Bioinformatics* **2015,** *31* (9), 1493-1495.
66. Trygg, J.; Wold, S., Orthogonal projections to latent structures (O-PLS). *Journal of Chemometrics* **2002,** *16* (3), 119-128.
67. Wishart, D. S.; Feunang, Y. D.; Marcu, A.; Guo, A. C.; Liang, K.; Vazquez-Fresno, R.; Sajed, T.; Johnson, D.; Li, C.; Karu, N.; Sayeeda, Z.; Lo, E.; Assempour, N.; Berjanskii, M.; Singhal, S.; Arndt, D.; Liang, Y.; Badran, H.; Grant, J.; Serra-Cayuela, A.; Liu, Y.; Mandal, R.; Neveu, V.; Pon, A.; Knox, C.; Wilson, M.; Manach, C.; Scalbert, A., HMDB 4.0: the human metabolome database for 2018. *Nucleic Acids Research* **2018,** *46* (D1), D608-D617.

68. Ulrich, E. L.; Akutsu, H.; Doreleijers, J. F.; Harano, Y.; Ioannidis, Y. E.; Lin, J.; Livny, M.; Mading, S.; Maziuk, D.; Miller, Z.; Nakatani, E.; Schulte, C. F.; Tolmie, D. E.; Wenger, R. K.; Yao, H.; Markley, J. L., BioMagResBank. *Nucleic Acids Research* **2008,** *36*, D402-D408.
69. Chong, J.; Wishart, D. S.; Xia, J., Using MetaboAnalyst 4.0 for Comprehensive and Integrative Metabolomics Data Analysis. *Current protocols in bioinformatics* **2019,** *68* (1), e86.
70. Kihira, S.; Tsankova, N. M.; Bauer, A.; Sakai, Y.; Mahmoudi, K.; Zubizarreta, N.; Houldsworth, J.; Khan, F.; Salamon, N.; Hormigo, A.; Nael, K., Multiparametric MRI texture analysis in prediction of glioma biomarker status: added value of MR diffusion. *Neuro-oncology advances* **2021,** *3* (1), vdab051-vdab051.
71. Bark, J. M.; Kulasinghe, A.; Chua, B.; Day, B. W.; Punyadeera, C., Circulating biomarkers in patients with glioblastoma. *British Journal of Cancer* **2020,** *122* (3), 295-305.
72. He, J.; Jiang, Y.; Liu, L.; Zuo, Z.; Zeng, C., Circulating MicroRNAs as Promising Diagnostic Biomarkers for Patients With Glioma: A Meta-Analysis. *Frontiers in Neurology* **2021,** *11*.
73. Kallenberg, K.; Bock, H. C.; Helms, G.; Jung, K.; Wrede, A.; Buhk, J.-H.; Giese, A.; Frahm, J.; Strik, H.; Dechent, P.; Knauth, M., Untreated Glioblastoma Multiforme: Increased Myo-inositol and Glutamine Levels in the Contralateral Cerebral Hemisphere at Proton MR Spectroscopy. *Radiology* **2009,** *253* (3), 805-812.
74. Ross, B. D.; Ernst, T.; Kreis, R.; Haseler, L. J.; Bayer, S.; Danielsen, E.; Bluml, S.; Shonk, T.; Mandigo, J. C.; Caton, W.; Clark, C.; Jensen, S. W.; Lehman, N. L.; Arcinue, E.; Pudenz, R.; Shelden, C. H., H-1 MRS in acute traumatic brain injury. *Journal of Magnetic Resonance Imaging* **1998,** *8* (4), 829-840.
75. Brooks, W. M.; Stidley, C. A.; Petropoulos, H.; Jung, R. E.; Weers, D. C.; Friedman, S. D.; Barlow, M. A.; Sibbitt, W. L.; Yeo, R. A., Metabolic and cognitive response to human traumatic brain injury: A quantitative proton magnetic resonance study. *Journal of Neurotrauma* **2000,** *17* (8), 629-640.
76. Hattingen, E.; Raab, P.; Franz, K.; Zanella, F. E.; Lanfermann, H.; Pilatus, U., Myo-Inositol: a marker of reactive astrogliosis in glial tumors? *NMR in Biomedicine* **2008,** *21* (3), 233-241.
77. Uhm, J. H.; Dooley, N. P.; Villemure, J. G.; Yong, V. W., Glioma invasion in vitro: Regulation by matrix metalloprotease-2 and protein kinase C. *Clinical & Experimental Metastasis* **1996,** *14* (5), 421-433.
78. da Rocha, A. B.; Mans, D. R. A.; Regner, A.; Schwartsmann, G., Targeting protein kinase C: New therapeutic opportunities against high-grade malignant gliomas? *Oncologist* **2002,** *7* (1), 17-33.
79. Castillo, M.; Smith, J. K.; Kwock, L., Correlation of myo-inositol levels and grading of cerebral astrocytomas. *American Journal of Neuroradiology* **2000,** *21* (9), 1645-1649.
80. Downes, C. P.; Macphee, C. H., Myoinositol Metabolites as cellular Signals. *European Journal of Biochemistry* **1990,** *193* (1), 1-18.
81. Moren, L.; Bergenheim, A. T.; Ghasimi, S.; Brannstrom, T.; Johansson, M.; Antti, H., Metabolomic Screening of Tumor Tissue and Serum in Glioma Patients Reveals Diagnostic and Prognostic Information. *Metabolites* **2015,** *5* (3), 502-520.
82. Steidl, E.; Pilatus, U.; Hattingen, E.; Steinbach, J. P.; Zanella, F.; Ronellenfitsch, M. W.; Baehr, O., Myoinositol as a Biomarker in Recurrent Glioblastoma Treated with Bevacizumab: A H-1-Magnetic Resonance Spectroscopy Study. *PLOS One* **2016,** *11* (12), e0168113.
83. Bouzier-Sore, A.-K.; Pellerin, L., Unraveling the complex metabolic nature of astrocytes. *Frontiers in Cellular Neuroscience* **2013,** *7*, 179.
84. Volkenhoff, A.; Weiler, A.; Letzel, M.; Stehling, M.; Klaembt, C.; Schirmeier, S., Glial Glycolysis Is Essential for Neuronal Survival in Drosophila. *Cell Metabolism* **2015,** *22* (3), 437-447.
85. Mashimo, T.; Pichumani, K.; Vemireddy, V.; Hatanpaa, K. J.; Singh, D. K.; Sirasanagandla, S.; Nannepaga, S.; Piccirillo, S. G.; Kovacs, Z.; Foong, C.; Huang, Z.; Barnett, S.; Mickey, B. E.; DeBerardinis, R. J.; Tu, B. P.; Maher, E. A.; Bachoo, R. M., Acetate Is a Bioenergetic Substrate for Human Glioblastoma and Brain Metastases. *Cell* **2014,** *159* (7), 1603-1614.
86. Bianchi, L.; De Micheli, E.; Bricolo, A.; Ballini, C.; Fattori, M.; Venturi, C.; Pedata, F.; Tipton, K. F.; Della Corte, L., Extracellular levels of amino acids and choline in human high grade gliomas: An intraoperative microdialysis study. *Neurochemical Research* **2004,** *29* (1), 325-334.
87. Ganapathy, V.; Thangaraju, M.; Prasad, P. D., Nutrient transporters in cancer: Relevance to Warburg hypothesis and beyond. *Pharmacology & Therapeutics* **2009,** *121* (1), 29-40.

88. Guntuku, L.; Naidu, V. G. M.; Yerra, V. G., Mitochondrial Dysfunction in Gliomas: Pharmacotherapeutic Potential of Natural Compounds. *Current Neuropharmacology* **2016,** *14* (6), 567-583.
89. Ordys, B. B.; Launay, S.; Deighton, R. F.; McCulloch, J.; Whittle, I. R., The Role of Mitochondria in Glioma Pathophysiology. *Molecular Neurobiology* **2010,** *42* (1), 64-75.
90. Natarajan, S. K.; Venneti, S., Glutamine Metabolism in Brain Tumors. *Cancers* **2019,** *11* (11), 1628.
91. Suh, E. H.; Hackett, E. P.; Wynn, R. M.; Chuang, D. T.; Zhang, B.; Luo, W.; Sherry, A. D.; Park, J. M., In vivo assessment of increased oxidation of branched-chain amino acids in glioblastoma. *Scientific Reports* **2019,** *9*, 340.
92. Toenjes, M.; Barbus, S.; Park, Y. J.; Wang, W.; Schlotter, M.; Lindroth, A. M.; Pleier, S. V.; Bai, A. H. C.; Karra, D.; Piro, R. M.; Felsberg, J.; Addington, A.; Lemke, D.; Weibrecht, I.; Hovestadt, V.; Rolli, C. G.; Campos, B.; Turcan, S.; Sturm, D.; Witt, H.; Chan, T. A.; Herold-Mende, C.; Kemkemer, R.; Koenig, R.; Schmidt, K.; Hull, W.-E.; Pfister, S. M.; Jugold, M.; Hutson, S. M.; Plass, C.; Okun, J. G.; Reifenberger, G.; Lichter, P.; Radlwimmer, B., BCAT1 promotes cell proliferation through amino acid catabolism in gliomas carrying wild-type IDH1. *Nature Medicine* **2013,** *19* (7), 901-908.
93. Ananieva, E. A.; Wilkinson, A. C., Branched-chain amino acid metabolism in cancer. *Current Opinion in Clinical Nutrition and Metabolic Care* **2018,** *21* (1), 64-70.
94. Tiwari, V.; Daoud, E. V.; Hatanpaa, K. J.; Gao, A.; Zhang, S.; An, Z.; Ganji, S. K.; Raisanen, J. M.; Lewis, C. M.; Askari, P.; Baxter, J.; Levy, M.; Dimitrov, I.; Thomas, B. P.; Pinho, M. C.; Madden, C. J.; Pan, E.; Patel, T. R.; DeBerardinis, R. J.; Sherry, A. D.; Mickey, B. E.; Malloy, C. R.; Maher, E. A.; Choi, C., Glycine by MR spectroscopy is an imaging biomarker of glioma aggressiveness. *Neuro-Oncology* **2020,** *22* (7), 1018-1029.
95. Tibbetts, A. S.; Appling, D. R., Compartmentalization of Mammalian Folate-Mediated One-Carbon Metabolism. In *Annual Review of Nutrition*, Cousins, R. J., Ed. 2010; Vol. 30, pp 57-81.
96. Jain, M.; Nilsson, R.; Sharma, S.; Madhusudhan, N.; Kitami, T.; Souza, A. L.; Kafri, R.; Kirschner, M. W.; Clish, C. B.; Mootha, V. K., Metabolite Profiling Identifies a Key Role for Glycine in Rapid Cancer Cell Proliferation. *Science* **2012,** *336* (6084), 1040-1044.
97. Zhang, W. C.; Shyh-Chang, N.; Yang, H.; Rai, A.; Umashankar, S.; Ma, S.; Soh, B. S.; Sun, L. L.; Tai, B. C.; Nga, M. E.; Bhakoo, K. K.; Jayapal, S. R.; Nichane, M.; Yu, Q.; Ahmed, D. A.; Tan, C.; Sing, W. P.; Tam, J.; Thirugananam, A.; Noghabi, M. S.; Pang, Y. H.; Ang, H. S.; Robson, P.; Kaldis, P.; Soo, R. A.; Swarup, S.; Lim, E. H.; Lim, B., Glycine Decarboxylase Activity Drives Non-Small Cell Lung Cancer Tumor-Initiating Cells and Tumorigenesis. *Cell* **2012,** *148* (1-2), 259-272.
98. Sreekumar, A.; Poisson, L. M.; Rajendiran, T. M.; Khan, A. P.; Cao, Q.; Yu, J.; Laxman, B.; Mehra, R.; Lonigro, R. J.; Li, Y.; Nyati, M. K.; Ahsan, A.; Kalyana-Sundaram, S.; Han, B.; Cao, X.; Byun, J.; Omenn, G. S.; Ghosh, D.; Pennathur, S.; Alexander, D. C.; Berger, A.; Shuster, J. R.; Wei, J. T.; Varambally, S.; Beecher, C.; Chinnaiyan, A. M., Metabolomic profiles delineate potential role for sarcosine in prostate cancer progression. *Nature* **2009,** *457* (7231), 910-914.
99. Locasale, J. W.; Grassian, A. R.; Melman, T.; Lyssiotis, C. A.; Mattaini, K. R.; Bass, A. J.; Heffron, G.; Metallo, C. M.; Muranen, T.; Sharfi, H.; Sasaki, A. T.; Anastasiou, D.; Mullarky, E.; Vokes, N. I.; Sasaki, M.; Beroukhim, R.; Stephanopoulos, G.; Ligon, A. H.; Meyerson, M.; Richardson, A. L.; Chin, L.; Wagner, G.; Asara, J. M.; Brugge, J. S.; Cantley, L. C.; Vander Heiden, M. G., Phosphoglycerate dehydrogenase diverts glycolytic flux and contributes to oncogenesis. *Nature Genetics* **2011,** *43* (9), 869–874.
100. Xia, Y.; Ye, B.; Ding, J.; Yu, Y.; Alptekin, A.; Thangaraju, M.; Prasad, P. D.; Ding, Z.-C.; Park, E. J.; Choi, J.-H.; Gao, B.; Fiehn, O.; Yan, C.; Dong, Z.; Zha, Y.; Ding, H.-F., Metabolic Reprogramming by MYCN Confers Dependence on the Serine-Glycine-One-Carbon Biosynthetic Pathway. *Cancer Research* **2019,** *79* (15), 3837-3850.
101. Vance, J. E.; Vance, D. E., Phospholipid biosynthesis in mammalian cells. *Biochemistry and Cell Biology* **2004,** *82* (1), 113-128.
102. Podo, F., Tumour phospholipid metabolism. *NMR in Biomedicine* **1999,** *12* (7), 413-439.
103. Herminghaus, S.; Pilatus, U.; Moller-Hartmann, W.; Raab, P.; Lanfermann, H.; Schlote, W.; Zanella, F. E., Increased choline levels coincide with enhanced proliferative activity of human neuroepithelial brain tumors. *NMR in Biomedicine* **2002,** *15* (6), 385-392.

104. Wright, A. J.; Fellows, G. A.; Griffiths, J. R.; Wilson, M.; Bell, B. A.; Howe, F. A., Ex-vivo HRMAS of adult brain tumours: metabolite quantification and assignment of tumour biomarkers. *Molecular Cancer* **2010,** *9*.
105. Hoxhaj, G.; Manning, B. D., The PI3K-AKT network at the interface of oncogenic signalling and cancer metabolism. *Nature Reviews Cancer* **2020,** *20* (2), 74-88.
106. Glunde, K.; Shah, T.; Winnard, P. T., Jr.; Raman, V.; Takagi, T.; Vesuna, F.; Artemov, D.; Bhujwalla, Z. M., Hypoxia regulates choline kinase expression through hypoxia-inducible factor-lot signaling in a human prostate cancer model. *Cancer Research* **2008,** *68* (1), 172-180.
107. Kinoshita, Y.; Yokota, A., Absolute concentrations of metabolites in human brain tumors using in vitro proton magnetic resonance spectroscopy. *NMR in Biomedicine* **1997,** *10* (1), 2-12.
108. Kinoshita, Y.; Yokota, A.; Koga, Y., Phosphorylethanolamine content of human brain tumors. *Neurologia medico-chirurgica* **1994,** *34* (12), 803-6.
109. Cuadrado, A.; Carnero, A.; Dolfi, F.; Jimenez, B.; Lacal, J. C., Phosphorylcholine - A novel 2nd messenger essential for mitogenic activity of growth-factors. *Oncogene* **1993,** *8* (11), 2959-2968.
110. Patel, A. B.; de Graaf, R. A.; Mason, G. F.; Rothman, D. L.; Shulman, R. G.; Behar, K. L., The contribution of GABA to glutamate/glutamine cycling and energy metabolism in the rat cortex in vivo. *Proceedings of the National Academy of Sciences of the United States of America* **2005,** *102* (15), 5588-5593.
111. Faria, A. V.; Macedo, F. C., Jr.; Marsaioli, A. J.; Ferreira, M. M. C.; Cendes, F., Classification of brain tumor extracts by high resolution H-1 MRS using partial least squares discriminant analysis. *Brazilian Journal of Medical and Biological Research* **2011,** *44* (2), 149-164.
112. El-Habr, E. A.; Dubois, L. G.; Burel-Vandenbos, F.; Bogeas, A.; Lipecka, J.; Turchi, L.; Lejeune, F.-X.; Coehlo, P. L. C.; Yamaki, T.; Wittmann, B. M.; Fareh, M.; Mahfoudhi, E.; Janin, M.; Narayanan, A.; Morvan-Dubois, G.; Schmitt, C.; Verreault, M.; Oliver, L.; Sharif, A.; Pallud, J.; Devaux, B.; Puget, S.; Korkolopoulou, P.; Varlet, P.; Ottolenghi, C.; Plo, I.; Moura-Neto, V.; Virolle, T.; Chneiweiss, H.; Junier, M.-P., A driver role for GABA metabolism in controlling stem and proliferative cell state through GHB production in glioma. *Acta Neuropathologica* **2017,** *133* (4), 645-660.
113. Yang, M.; Pollard, P. J., Succinate: A New Epigenetic Hacker. *Cancer Cell* **2013,** *23* (6), 709-711.
114. Selak, M. A.; Armour, S. M.; MacKenzie, E. D.; Boulahbel, H.; Watson, D. G.; Mansfield, K. D.; Pan, Y.; Simon, M. C.; Thompson, C. B.; Gottlieb, E., Succinate links TCA cycle dysfunction to oncogenesis by inhibiting HIF-alpha prolyl hydroxylase. *Cancer Cell* **2005,** *7* (1), 77-85.
115. Xiao, M.; Yang, H.; Xu, W.; Ma, S.; Lin, H.; Zhu, H.; Liu, L.; Liu, Y.; Yang, C.; Xu, Y.; Zhao, S.; Ye, D.; Xiong, Y.; Guan, K.-L., Inhibition of alpha-KG-dependent histone and DNA demethylases by fumarate and succinate that are accumulated in mutations of FH and SDH tumor suppressors. *Genes & Development* **2012,** *26* (12), 1326-1338.
116. Laukka, T.; Mariani, C. J.; Ihantola, T.; Cao, J. Z.; Hokkanen, J.; Kaelin, W. G., Jr.; Godley, L. A.; Koivunen, P., Fumarate and Succinate Regulate Expression of Hypoxia-inducible Genes via TET Enzymes. *The Journal of biological chemistry* **2016,** *291* (8), 4256-65.
117. Letouzé, E.; Martinelli, C.; Loriot, C.; Burnichon, N.; Abermil, N.; Ottolenghi, C.; Janin, M.; Menara, M.; Nguyen, A. T.; Benit, P.; Buffet, A.; Marcaillou, C.; Bertherat, J.; Amar, L.; Rustin, P.; De Reyniès, A.; Gimenez-Roqueplo, A. P.; Favier, J., SDH mutations establish a hypermethylator phenotype in paraganglioma. *Cancer Cell* **2013,** *23* (6), 739-52.
118. Killian, J. K.; Kim, S. Y.; Miettinen, M.; Smith, C.; Merino, M.; Tsokos, M.; Quezado, M.; Smith, W. I., Jr.; Jahromi, M. S.; Xekouki, P.; Szarek, E.; Walker, R. L.; Lasota, J.; Raffeld, M.; Klotzle, B.; Wang, Z.; Jones, L.; Zhu, Y.; Wang, Y.; Waterfall, J. J.; O'Sullivan, M. J.; Bibikova, M.; Pacak, K.; Stratakis, C.; Janeway, K. A.; Schiffman, J. D.; Fan, J. B.; Helman, L.; Meltzer, P. S., Succinate dehydrogenase mutation underlies global epigenomic divergence in gastrointestinal stromal tumor. *Cancer discovery* **2013,** *3* (6), 648-57.
119. Brooks, G. A., The Science and Translation of Lactate Shuttle Theory. *Cell Metab* **2018,** *27* (4), 757-785.
120. San-Millán, I.; Brooks, G. A., Reexamining cancer metabolism: lactate production for carcinogenesis could be the purpose and explanation of the Warburg Effect. *Carcinogenesis* **2017,** *38* (2), 119-133.

121. de la Cruz-López, K. G.; Castro-Muñoz, L. J.; Reyes-Hernández, D. O.; García-Carrancá, A.; Manzo-Merino, J., Lactate in the Regulation of Tumor Microenvironment and Therapeutic Approaches. *Frontiers in oncology* **2019,** *9*, 1143.
122. Bhagat, T. D.; Von Ahrens, D.; Dawlaty, M.; Zou, Y. Y.; Baddour, J.; Achreja, A.; Zhao, H. Y.; Yang, L. F.; Patel, B.; Kwak, C.; Choudhary, G. S.; Gordon-Mitchell, S.; Aluri, S.; Bhattacharyya, S.; Sahu, S.; Bhagat, P.; Yu, Y. T.; Bartenstein, M.; Giricz, O.; Suzuki, M.; Sohal, D.; Gupta, S.; Guerrero, P. A.; Batra, S.; Goggins, M.; Steidl, U.; Greally, J.; Agarwal, B.; Pradhan, K.; Banerjee, D.; Nagrath, D.; Maitra, A.; Verma, A., Lactate-mediated epigenetic reprogramming regulates formation of human pancreatic cancer-associated fibroblasts. *Elife* **2019,** *8*, e50663.
123. Zhang, D.; Tang, Z.; Huang, H.; Zhou, G.; Cui, C.; Weng, Y.; Liu, W.; Kim, S.; Lee, S.; Perez-Neut, M.; Ding, J.; Czyz, D.; Hu, R.; Ye, Z.; He, M.; Zheng, Y. G.; Shuman, H. A.; Dai, L.; Ren, B.; Roeder, R. G.; Becker, L.; Zhao, Y., Metabolic regulation of gene expression by histone lactylation. *Nature* **2019,** *574* (7779), 575-580.
124. El Hassouni, B.; Granchi, C.; Valles-Marti, A.; Supadmanaba, I. G. P.; Bononi, G.; Tuccinardi, T.; Funel, N.; Jimenez, C. R.; Peters, G. J.; Giovannetti, E.; Minutolo, F., The dichotomous role of the glycolytic metabolism pathway in cancer metastasis: Interplay with the complex tumor microenvironment and novel therapeutic strategies. *Seminars in Cancer Biology* **2020,** *60*, 238-248.
125. Bushunow, P.; Reidenberg, M. M.; Wasenko, J.; Winfield, J.; Lorenzo, B.; Lemke, S.; Himpler, B.; Corona, R.; Coyle, T., Gossypol treatment of recurrent adult malignant gliomas. *Journal of Neuro-Oncology* **1999,** *43* (1), 79-86.

126. Daniele, S.; Giacomelli, C.; Zappelli, E.; Granchi, C.; Trincavelli, M. L.; Minutolo, F.; Martini, C., Lactate dehydrogenase-A inhibition induces human glioblastoma multiforme stem cell differentiation and death. *Scientific Reports* **2015,** *5*, 15556.